Robust video transmission over lossy channels and efficient video distribution over peer-to-peer networks

Jiajun Wang

Electrical Engineering and Computer Sciences
University of California at Berkeley

Technical Report No. UCB/EECS-2008-152
http://www.eecs.berkeley.edu/Pubs/TechRpts/2008/EECS-2008-152.html

December 10, 2008

Robust video transmission over lossy channels and efficient video distribution over peer-to-peer networks

by

Jiajun Wang

B.S. (University of Illinois at Urbana-Champaign) 2003
M.S. (University of California, Berkeley) 2006

A dissertation submitted in partial satisfaction of the
requirements for the degree of
Doctor of Philosophy

in

Engineering - Electrical Engineering and Computer Sciences

and the Designated Emphasis

in

Communication, Computation and Statistics

in the

GRADUATE DIVISION
of the
UNIVERSITY of CALIFORNIA, BERKELEY

Committee in charge:

Professor Kannan Ramchandran, Chair
Professor Avideh Zakhor
Professor Bruno Olshausen

Fall 2008

Abstract

Robust video transmission over lossy channels and efficient video distribution over peer-to-peer networks

by

Jiajun Wang

Doctor of Philosophy in Engineering - Electrical Engineering and Computer Sciences and the Designated Emphasis in Communication, Computation and Statistics

University of California, Berkeley

Professor Kannan Ramchandran, Chair

Though technologies for video compression and client-server based video distribution have matured, applications fueled by recent development of communication networks pose new challenges. In this dissertation, we study two classes of video applications.

The first class is low-latency video streaming over lossy networks. Today's dominant codecs based on motion-compensated predictive coding, such as MPEG, can compress videos efficiently. However, the decoded video quality is susceptible to transmission packet losses, which occur frequently over both the Internet and cellular networks. In order to enable robust low-latency video transmission, we adopt a video coding framework based on information-theoretical principles of distributed source coding. We present the theoretical foundation of a distributed source coding based video codec as well as the practical implementations. Extensive simulations demonstrate the superiority of the proposed codec over conventional robustness-enhancing methods, such as intra refresh and forward error correction codes.

The second class is video distribution over peer-to-peer (P2P) overlay networks. Compared to the traditional client-server architecture, P2P technologies can offer tremendous scalability and greatly reduce server cost. Due to the bandwidth asymmetry experienced by Internet users, however, P2P systems are oftentimes bottlenecked by users' limited upload bandwidth. We propose to ease the bottleneck by utilizing Internet users with spare upload capacity, whom we term helpers. We present a light-weight helper protocol that is backwards-compatible with the popular BitTorrent protocol and analyze the steady-state system performance. We verify the efficiency and effectiveness of the proposed protocol and the accuracy of the analysis through extensive simulations. We further extend the philosophy for live video streaming. We use a simple fluid-level analysis to guide our system design. We demonstrate that the simple analysis provides a good estimate of system performance and verify that the proposed system can efficiently utilize helpers' upload bandwidth even with high peer churning through extensive simulations.

Professor Kannan Ramchandran
Dissertation Committee Chair

Contents

List of Figures

Acknowledgements

I wish to acknowledge my deep debt of gratitude to my advisor and thesis committee chair Prof. Kannan Ramchandran for his guidance, support and encouragement throughout the course of my graduate study. This research would not have been possible without his vision and motivation.

I am extremely grateful to the other members of my dissertation committee Professor Zakhor and Professor Olshausen who also served on my qualifying exam committee for their invaluable feedback on this dissertation. I would like to thank my colleagues Abhik Majumdar, Vinod Prabhakaran, Alex Dimakis, and Chuohao Yeo for their invaluable help at various stages of my research and for the many productive discussions that we had. I would also like to thank everyone from the Collaboration and Communication Systems group at Microsoft Research, especially Minghua Chen, Cheng Huang and Jin Li, for a fulfilling research experience.

I would like to thank all my friends at Berkeley and all the members of the BASiCS group and Wireless Foundations for making my stay at Berkeley a memorable and enjoyable one.

My parents have been a constant source of encouragement without whose love and support I would not have been able to make it this far. I am deeply indebted to them.

Chapter 1

Introduction

With the explosive development of communication networks, demand for multimedia applications has grown not only in quantity but also in variety and quality. Consumers are no longer content to watching TV over cable networks or DVDs from Blockbuster. Now there is demand to download and watch high definition movies over the Internet, watch live sports broadcast using our laptops, have a video conference using our cell phones, and watch high-quality videos on YouTube. In this dissertation, we focus on two important classes of video applications.

In Part I, we consider the problem of low-latency video streaming over packet networks characterized by bursty losses, such as wireless networks. In particular, we focus on applications characterized by stringent end-to-end delay constraints that are of the order of a fraction of a second.[1] Examples include video telephony, interactive distance learning, and video surveillance. Compared to traditional wireline networks, today's dominant transmission channels, such as WiFi and cellular net-

[1]A necessary requirement for conversational services is for end-to-end delay to be less than 250 milliseconds[44].

works, are prone to transmission errors. As a result, in addition to the conventional requirement of high compression efficiency, such applications require the compressed bitstream to be robust to packet losses caused by transmission errors. These requirements need to be met *simultaneously* and *under stringent delay constraints*.

While today's popular video coders, such as MPEG-x and H.26x [25, 15, 9, 10, 48], can compress video signals efficiently, the compressed bitstream is susceptible to packet losses. This is a direct consequence of the motion-compensated predictive coding (MCPC) framework that underlies these codecs. Conventional approaches, such as automatic repeat-request (ARQ) [28] and forward error correction codes (FEC) [29], focus on ensuring that the decoder receive the entire compressed bitstream, either through retransmission or error-correcting decoding. These are very effective techniques for scenarios involving independent packet losses and more lenient end-to-end delay constraints. However, wireless transmission media are characterized by bursty packet drops. This unique attribute makes low-latency streaming applications highly challenging.

We take an alternative approach and present a video coding framework based on information theoretical principles of distributed source coding (DSC) [43, 50]. Instead of guaranteeing delivery of every data packet, the proposed codec allows occasional frame corruptions due to bursty packet drops. Instead, it arrests the effect of such frame corruptions immediately in the following frames, thus maintaining high visual quality. We summarize our contributions in this part of this thesis as follows.

- On the theoretical side, we illustrate the proposed method through a simple but conceptually illustrative model. This analytically tractable model captures the essence of the dynamics related to transmitting temporally dependent source information over packet erasure channels. Under certain modeling assumptions, we quantify the performance gains of the proposed distributed source coding based video codec over a conventional predictive coding system, such as MPEGx/H.26x, when the video stream is transmitted over a lossy channel.

- Building on the insights from the theoretical model, we implement a practical video coding system. We present extensive simulation results, which demonstrate the strengths and weaknesses of the proposed system over standard approaches, such as protecting predictively coded bitstream with FEC codes and random intra refresh.

In Part II, we focus on video distribution over peer-to-peer (P2P) networks. Video distribution over Internet using the traditional client-server method places tremendous burden on existing infrastructure, such as data centers and content distribution networks (CDN). In fact, the existing client-server infrastructure lacks the scalability to support an increasingly large user base due to limited backbone capacity [5]. P2P-based Internet video distribution, both download and streaming applications, can greatly reduce server bandwidth costs of content providers and bypass bottlenecks between providers and consumers. In a P2P content distribution network, peers interested in the same content form an overlay network. The content of interest is broken into pieces. Peers upload and download these pieces simultaneously among themselves thus offloading server burden by utilizing the upload bandwidth of participating peers.

There are many aspects to improving a P2P network. In Chapter 6 of the dissertation, we focus on easing the bottleneck of P2P network performance caused by the asymmetry of today's Internet connections. Specifically, we study how to improve the performance of P2P networks for video download and multicast through a higher level of collaboration among peers. The system throughput of a P2P network is capped by the smaller one between the total system upload bandwidth and the total system download bandwidth [38]. However, a large population of Internet users today have highly asymmetric Internet connections, such as ADSL and cable, and have much lower upload than download bandwidth. As a result, peers' total available upload capacity often becomes the most dominant constraint of a P2P network.

We propose to overcome this constraint by promoting a higher level of collaboration among network peers to optimize performance of uplink-scarce collaborative networks beyond what can be achieved by conventional P2P networks. One important observation is that at any given time, while there are peers exhausting their upload bandwidth sharing data, there are also numerous peers with spare upload capacity. This is a direct result of the statistical multiplexing property of a large-scale system in the sense that peers have not only different physical capabilities but also different behavioral characteristics. We call such peers *helpers*. Helpers represent a rich untapped resource, whose upload bandwidth can be exploited to increase the total system upload bandwidth and hence ease the performance bottleneck. We study the efficient use of helpers for P2P video download and extend the philosophy to live video multicast. We make the following contributions.

- For video download, we use average peer download time as the performance metric and develop a distributed helper protocol that is backwards-compatible with the popular BitTorrent file sharing protocol [14]. We analyze steady-state system performance using a modified version of the fluid model of Qiu and Srikant [38], and also make corrections to the analysis presented there. We demonstrate both analytically and empirically that helpers' upload bandwidth can be efficiently utilized using the proposed protocol and verify the accuracy of the fluid model analysis.

- For live multicast, we aim to minimize server load of a P2P live multicast system in which peers' average upload bandwidth is smaller than video bitrate. We use a simple first-order analysis to derive the performance upper bound and use it to guide the design of a constructive solution. We show through extensive simulation that the proposed strategy can closely match this performance bound.

Part I

Robust video transmission over lossy networks

Chapter 2

Motivation and background

Real-time video transmission over lossy networks is an area that has been widely studied by both academia and industry. Two of the main reasons are:

- Today's popular transmission media, such as the Internet and cellular networks, are prone to transmission packet losses;
- Though today's popular video coders, such as MPEG-x and H.26x [25, 15, 9, 10, 48], can compress videos efficiently, the compressed bitstream is susceptible to packet losses.

The fragility of MPEG-like compressed bitstream is a direct consequence of the predictive coding framework that underlies these codecs. At a high level, each frame of the video is divided into non-overlapping blocks. Each encoding block is "matched" with the most similar block in the previous frame, called predictor block. Only the difference between the two blocks is encoded. In other words, each block is *deterministically* associated with one single predictor. If that predictor is corrupted due to channel loss, there will be a predictor mismatch between encoder and decoder. When this happens, even if the difference between the current block and the predictor block is correctly received, the reconstruction will still be erroneous. This error will propagate until the next independently encoded frame is decoded, causing severe visual quality degradation.

A number of novel ideas and useful tools have been developed to enable robust transmission of predictively encoded video bitstreams, including automatic repeat request (ARQ) [28], forward error correction codes (FEC) [29], and a combination of the two (hybrid ARQ), etc. These techniques focus on ensuring that the decoder receive the entire compressed bitstream. They are very effective with independent packet drops and more lenient constraints on end-to-end delay.

We focus on a class of applications with stringent end-to-end delay constraints that are of the order of a fraction of a second. Examples include video telephony, interactive distance learning, and video surveillance. Further, wireless transmission media are characterized by bursty packet drops. These unique characteristics make the problem especially challenging, compared to regular video-streaming applications, which can allow up to tens of seconds of buffering.

We propose to take an alternative approach and present a video coding framework based on information theoretical principles of distributed source coding (DSC) [43, 50]. Instead of trying to recover every data packet, the proposed codec allows frames transmitted under poor channel condition to be corrupted, but arrests the effect of packet drops immediately in the following frames. Specifically, we aim to recover a block even if the predictor block at the decoder is corrupted and cannot be predicted at the encoder. This is possible because in the DSC framework, each encoding block is no longer encoded based on a single predictor in a *deterministic* fashion, e.g. via differential coding. Instead, each block is encoded based on the *statistical* correlation between the block and the best predictor available at the decoder using channel coding techniques. Once a block is channel coded targeting a specific correlation, *any* predictor at the decoder that is sufficiently correlated with the current block can be used to decode the block correctly. Using the terminology of information theory, the current block to be encoded is called the source, and the candidate predictor used for decoding is called the *side information*.

There are two important aspects of using distributed source coding framework. First, the decoder needs to have a high-quality side information. Second, the encoder needs to be able to accurately estimate the correlation between the current block and the side information. In the scenario of video streaming over lossy channel, as video data is highly non-stationary, correlation estimation in the presence of unpredictable channel noise remains a challenging open question in general. In this work, we propose a video coding system that carries out a joint side information selection and correlation estimation scheme. By doing this and following a joint source-channel coding approach, the proposed DSC-based codec can efficiently tune to both the source content as well as to the network loss characteristics while respecting stringent latency constraints.

2.1 Video coding and distributed source coding background

We review background knowledge on both the predictive video coding architecture and principles of distributed source coding so that we can better understand the fragility of predictively encoded video bitstreams in the face of transmission errors and the theoretical foundation underlying the proposed system.

2.1.1 Predictve video coding background

First, we present a quick overview of the conventional motion-compensated predictive video coding architecture that underlies current video coding standards such as the MPEG-x and H.26x standards.

A video sequence is a collection of images (also called pictures, frames) in time. Uncompressed video data contain both spatial and temporal redundancy. Spatial redundancy can be reduced through applying Discrete Cosine Transform (DCT) to the images while temporal redundancy is typically reduced through motion compensation. For the purpose of encoding, each of these frames is decomposed into a grid of non-overlapping blocks. These blocks are encoded primarily in the following two modes to exploit spatial and/or temporal redundancy.

1. **Intra-Coding (I) Mode:** The intra-coding mode exploits only the spatial correlation in the frame by using the Discrete Cosine Transform (DCT) to each block that is intra-coded. It typically has poor compression efficiency, since it does not exploit the temporal redundancy in a video sequence.

2. **Inter-Coding or Motion Compensated Predictive (P) Mode:** In con-

trast to the intra-coding mode, this mode exploits both the spatial and temporal correlation present in the video sequence resulting in highly efficient compression. The motion estimation operation looks in the frame memory to find the best predictor block for the block being encoded. A motion vector is produced in this process to indicate the location of the best predictor. The residue between the predictor block and the current block being encoded, also called Displaced Frame Difference (DFD), is then transformed into DCT domain and encoded. Figure 2.1 illustrates the inter-coding operation.

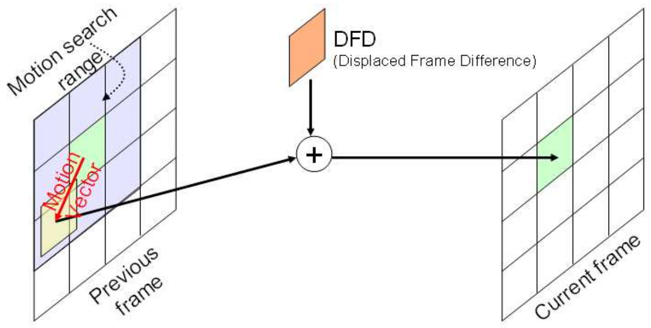

Figure 2.1: Simplified demonstration of motion compensated predictive coding. Each frame is broken into non-overlapping blocks. To encode each block, the best predictor block is located within a search range in the reference. The displacement between the current block and the predictor block is called motion vector. Only the difference between the current block and the predictor block and the motion vector are transmitted.

Typically, the video sequence is grouped into a Group of Pictures (GOP) (see Figure 2.2) where every block in the first frame (I-frame) of a GOP is coded in Intra-mode while blocks in the remaining frames (P-frame's) of the GOP are usually coded in Inter-mode (though some of the blocks within a P-frame may be coded in Intra-mode). Figure 2.3, 2.4 are block diagrams of typical predictive encoder and

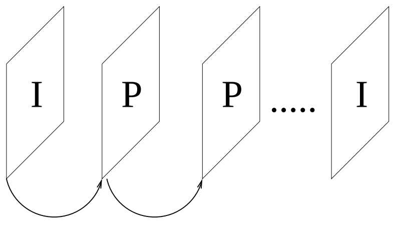

Figure 2.2: An example of a group of pictures (GOP). Every GOP starts with an I-frame. It is followed by a serious of P or B-frames.

decoder.

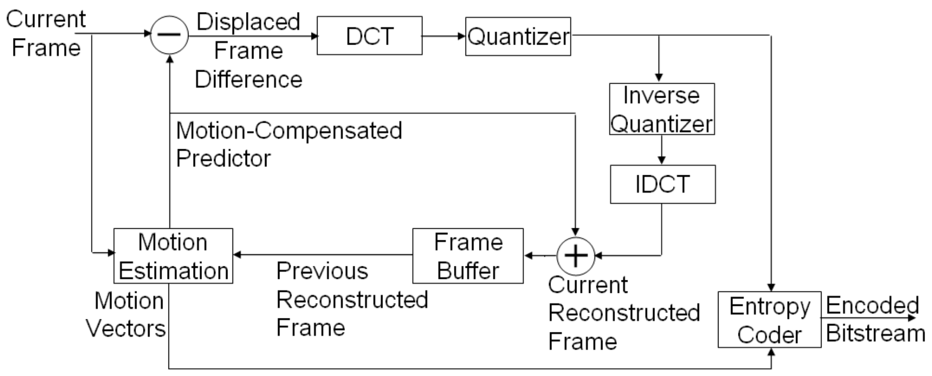

Figure 2.3: Block diagram for a typical predictive encoder. The main components include motion search, decorrelating transform, quantization and entropy coding.

While motion compensated predictive coding achieves very efficient compression through exploiting both temporal and spatial redundancy, it suffers from a drawback: fragility to loss of synchronization (or “drift”) between encoder and decoder in the face of prediction mismatch, e.g., due to channel loss. When the frame memory “state” at encoder and decoder differs, e.g. due to packet drops, the residue error is encoded at the encoder off one predictor and decoded at the decoder off a different (corrupted) predictor. Once this error happens, it will prop-

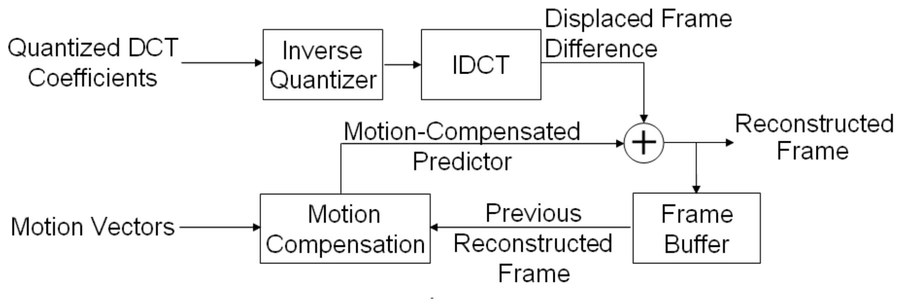
Quantized DCT Coefficients
Inverse Quantizer
IDCT
Displaced Frame Difference
Reconstructed Frame
Motion-Compensated Predictor
Motion Vectors
Motion Compensation
Previous Reconstructed Frame
Frame Buffer

Figure 2.4: Block diagram for a typical predictive decoder. The main components include entropy decoding, inverse quantization, inverse transform and motion compensation.

agate until intra-coded blocks replace the blocks in error, causing drift. This loss of synchronization leads to a significant degradation in the decoded video quality. In practice, the decoded quality often continues to deteriorate till the next intra-frame is received. This problem is exacerbated in wireless communication environments, which are characterized by bursty packet drops.

2.1.2 Error-resilient video transmission

Without changing the encoded bitstream, the two most basic approaches to enable error-resilient video streaming are automatic repeat-request (ARQ) [28] and forward error correction coding (FEC) [29].

Automatic Repeat-reQuest (ARQ) is an error control method for data transmission which uses acknowledgments and timeouts to achieve reliable data transmission. The basic idea is to have the receiver send an acknowledgment (ACK) message to the transmitter to indicate that it has correctly received a data packet. If the sender does not receive an ACK before a timeout period, it retransmits the packet until it receives an ACK or exceeds a predefined number of re-transmissions. To enable ARQ, a feedback channel is required. The lower the feedback channel delay is, the better the performance.

In telecommunication and information theory, forward error correction (FEC) is a system of error control for data transmission, whereby the sender adds redundant data to its messages, also known as an error correction code. This allows the receiver to detect and correct errors (within some bound) without the need to ask the sender for additional data. The advantage of FEC over ARQ is that a feedback channel is not required, or that retransmission of data can often be avoided, at the cost of higher bandwidth requirements on average. FEC is therefore applied in situations where retransmissions are relatively costly or impossible.

In the context of transmission over lossy channels, block codes are typically used. Block codes work on fixed-size blocks, or packets, of bits or symbols. A file is broken into k pieces of equal size and encoded into n $(n > k)$ coded pieces. Among all block codes, the maximum-distance separable (MDS) ones are optimal in terms of minimum redundancy. An (n, k) MDS erasure code can correct up to $n - k$ erasures. This means if the sender breaks the file into k pieces and transmit n MDS-coded packets, as long as the receiver receives at least k of them, it can completely reconstruct the original file. Reed-Solomon (RS) codes are the most notable class of MDS codes because of its widespread use on the Compact disc, the DVD, and in computer hard drives. We will assume RS codes whenever we use FEC codes in the rest of the thesis.

ARQ and FEC share the goal of successfully transmitting every packet and perfectly reconstructing the source. This is indeed very important for predictively coded video bitstream because the encoder and decoder need to be synchronized. Without any delay constraint, both ARQ and FEC are optimal. However, the stringent delay constraint posed by the applications of interest render these approaches much less effective. For ARQ, when the delay constraint is stringent, no retransmission may be possible before an erroneously decoded frame has to be displayed. This will cause error propagation until retransmission and re-decoding completes. For FEC, if any of the k data packets gets dropped during transmission, we have to receive k packets before we can recover the lost data packets. The delay constraint thus bounds the number of packets k that we can group together to apply FEC codes. Given a target decoding probability and a fixed packet drop probability, we need a larger rate overhead, i.e. $\frac{n-k}{k}$, for a smaller k. This overhead can become significant if the transmission packet drops are not independent and instead have a bursty nature, such as wireless channels. While this overhead can be tolerated for low-latency audio transmission, the high rate nature of video data makes this approach much less desirable given limited transmission bandwidth.

Another approach to enable robust video transmission is to alter the encoding process. The most basic and common approach is to increase the number of blocks that are intra-encoded in a predictively coded frame. As we reviewed earlier, intra-coded blocks do not rely on any previous blocks. Thus even if a reference frame is corrupted, the intra-coded blocks in the following frame will be correctly reconstructed, thereby stopping drift in those blocks.

Our approach is more similar to intra refresh. Intra refresh is an error-resilience technique where blocks outside of I-frames are intra-coded and transmitted from time to time to arrest the effect of error propagation. Like intra-refresh, we also do not attempt to recover every dropped packet. Instead, we aim to arrest the effect of packet drops immediately after. However, the proposed scheme is much more compression-efficient in that it makes use of the temporal correlation between the current block and predictors in possibly corrupted erroneous frames.

The following section provides an overview of a particular setup of distributed source coding that is of interest: source coding with side-information. The key concepts will be illustrated through examples to provide intuition on why the framework of distributed source coding is potentially beneficial for transmission with losses.

2.1.3 Distributed source coding background

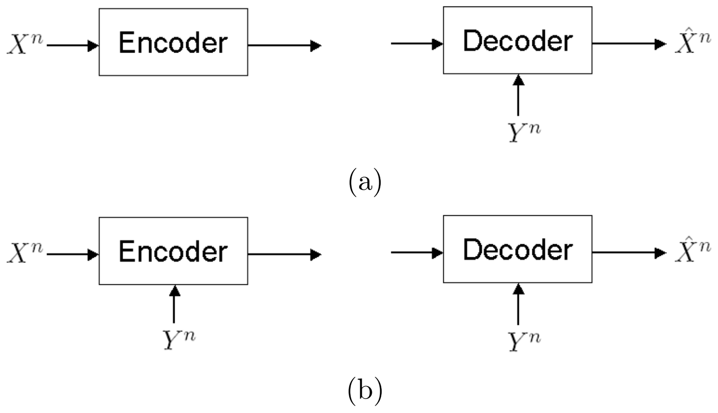

Figure 2.5: $\{X_i, Y_i\}_{i=1}^n$ are i.i.d. with joint probability distribution $p(x, y)$. $\hat{X}^n$ is the decoder reconstruction of X^n. (a) Source Coding with Side-Information only at the decoder. (b) Source Coding with Side-Information at both encoder and decoder.

Consider the problems depicted in Figures 2.5(a) and (b). $\{X_i, Y_i\}_{i=1}^n$ are i.i.d. with joint probability distribution $p(x, y)$. $\hat{X}^n$ is the decoder reconstruction of

X^n. The objective is to recover X^n at the decoder to within a distortion constraint D for some distortion measure $d(x, \hat{x})$. In Figure 2.5(a), the side-information Y^n is available only to the decoder, while in Figure 2.5(b) it is available to both encoder and decoder. The problem of Figure 2.5(a) is often referred to as source coding with side-information.

Lossless coding case

For lossless coding with finite alphabets, the decoder is interested in recovering X^n perfectly with high probability, i.e.

$$P_e^{(n)} = P(\hat{X}^n \neq X^n) \to 0 \quad \text{as} \quad n \to \infty$$

From information theory [16] we know that the rate region for the problem of Figure 2.5(b), when the side-information is available to both encoder and decoder, is $R \geq H(X|Y)$. When the distortion measure $d(\cdot, \cdot)$ is Hamming distance and the desired distortion $D = 0$, this becomes a version of the problem solved by Slepian and Wolf [43]. The surprising result of Slepian and Wolf [43] is that the rate region for the problem of Figure 2.5(a), when the side-information is only available to the decoder, is also $R \geq H(X|Y)$. *Thus one can do as well when the side-information is available only to the decoder as when it is available to both encoder and decoder.* To do this, the space of all X^n sequences is randomly partitioned, or *binned*, into $2^{nH(X|Y)}$ *cosets*, each containing an equal number of sequences. The encoder indicates which coset the source realization X^n lies in. Slepian and Wolf showed that with high probability, the decoder is able to identify the correct X^n in the indicated coset using the side information Y^n. To better understand the idea of binning, it is instructive to examine the following example from [36].

Illustrative Example for Slepian-Wolf Coding: Let X and Y be length 3-bit binary data that can equally likely take on each of the 8 possible values. X and Y are correlated such that the Hamming distance between them is at most 1. That is, given Y (e.g., [0 1 0]), X is either the same as Y ([0 1 0]) or differs in one of the three bits ([1 1 0], [0 0 0] or [0 1 1]). The goal is to efficiently encode X in the two scenarios depicted in Figures 2.5(a) and (b) so that it can be perfectly reconstructed at the decoder. Information theory prescribes that we cannot hope to compress X to fewer than 2 bits as $H(X|Y) = 2$. We will now explain how this can be achieved in both of the scenarios in Figure 2.5.

Scenario 1: In the first scenario (see Figure 2.5(b)), Y is present both at the encoder and at the decoder. The encoder can simply calculate the residue $X \oplus Y$ and send the information. Since there are only four possible values of $X \oplus Y$ ([0 0 0], [0 0 1], [0 1 0] and [1 0 0]), the encoder only needs to send 2 bits to signal the value. The decoder will then recover X through $X \oplus Y \oplus Y$. In the context of video coding, X is analogous to the current video block that is being encoded, Y is analogous to the motion-compensated predictor from the frame memory, the residue between X and Y is analogous to the displaced frame difference, hence this mode of encoding is similar to *predictive coding.*

Scenario 2: In this setup, Y is made available only to the decoder (see Figure 2.5(a)). The encoder for X does not have access to Y but it does know the correlation structure between X and Y and also the fact that the decoder has access to Y. Since this scenario is strictly not better than the first scenario, its performance is limited by that of the first scenario. However, from the Slepian-Wolf theorem [43] we know that even in this seemingly worse case, we can achieve the same performance as in the first scenario (i.e. encode X using 2 bits).

This can be done using the following approach. The space of possible values (codewords) of X is partitioned into 4 sets (called cosets) each containing 2 codewords, namely, **Coset 1** ([0 0 0] and [1 1 1]), **Coset 2** ([0 0 1] and [1 1 0]), **Coset 3** ([0 1 0] and [1 0 1]) and **Coset 4** ([1 0 0] and [0 1 1]). The encoder for X identifies the coset containing the codeword for X and sends the index for the coset in 2 bits instead of the actual codeword. The decoder, in turn, upon receiving the coset index, uses Y to disambiguate the correct X from the set by declaring the codeword that is closest to Y as the answer. Note that this is feasible because the distance between X and Y is at most 1, while the distance between the two codewords in any set is 3.

We note that **Coset 1** in the above example is a repetition channel code [29] of distance 3 and the other sets are cosets [19, 20] of this code in the codeword space of X. In channel coding terminology, each coset is associated with an unique index, called *syndrome*. We have used a channel code that is "matched" to the correlation distance (or equivalently, noise) between X and Y to partition the source codeword space of X (which is the set of all possible 3 bit words) into cosets of the 3-bit repetition channel code. The decoder here needs to perform *channel decoding* since it needs to identify the source codeword from the list of codewords enumerated in the coset indicated by the encoder. To do so, it finds the codeword in the signalled coset that is closest to Y. Since the encoder sends the index or *syndrome* for the coset containing the codeword for X to the decoder, we sometimes refer to this operation as **syndrome coding**.

We now compare Scenario 1 and 2 and demonstrate the inherent robustness of the distributed source coding framework. Let Y be [0 0 0] and X be [0 0 1]. Under

Scenario 1, we use two bits to indicate to the decoder that $X \oplus Y = [010]$. If for some reason Y at decoder gets corrupted and becomes [0 0 1], the decoder will decode X to be $[0\ 0\ 1] \oplus [0\ 1\ 0] = [0\ 1\ 1]$, which is incorrect. Under Scenario 2, on the other hand, we use two bits to indicate that X belones to **Coset 2** ([0 0 1] and [1 1 0]). Now, if Y becomes [0 0 1] accidentally, the decoder will still decode X to be [0 0 1] as this is the codeword closest to the side information Y under Hamming distortion. In fact, if as long as Y remains within Hamming distance 1 to X, decoding will always succeed.

We now turn to the case when we are interested in recovering X^n at the decoder to within some distortion.

Lossy coding case

Consider again the problem of Figure 2.5(a). We now remove the constraint on X and Y to be discrete and allow them to be continuous random variables as well. We are now interested in recovering X^n at the decoder to within a distortion constraint D for some distortion measure $d(x, \hat{x})$. Let $\{X_i, Y_i\}_{i=1}^n$ be i.i.d. with joint probability distribution $p(x, y)$ and let the distortion measure be $d(x^n, \hat{x}^n) = \frac{1}{n}\sum_{i=1}^n d(x_i, \hat{x}_i)$. Then the Wyner-Ziv theorem [50] states that the rate distortion function for this problem is

$$R(D) = \min_{p(u|x)p(\hat{x}|u,y)} I(X;U) - I(Y;U)$$

where

$$p(x, y, u) = p(u|x)p(x, y)$$

and the minimization is under the distortion constraint

$$\sum_{x,u,y,\hat{x}} p(\hat{x}|u,y)p(u|x)p(x,y)d(x,\hat{x}) \leq D$$

Here U is the active source codeword and the term $I(Y;U)$ is the rate rebate due to the presence of the side-information at the decoder.

For the case when X and Y are jointly Gaussian and the mean squared error is the distortion measure, it can be shown, using the Wyner-Ziv theorem [50], that the rate-distortion performance for coding X^n is the same whether or not the encoder has access to Y^n. In other words, for this case, the performance of the system depicted in Figure 2.5(a) can again match that of Figure 2.5(b).

Let us illustrate the concept of coset binning for lossy source coding through the following example. Let X be a scalar real-valued number that the encoder is trying to communicate to the decoder within distortion $\pm\frac{\Delta}{2}$. The decoder has access to side information Y. Y is a noisy version of X, and can be expressed as $Y = X + N$ where N is the correlation noise. In this example, we assume that X and Y are correlated such that $|N| = |Y - X| < \frac{3\Delta}{2}$. The encoder first quantizes X to $\hat{X}$ with a scalar quantizer with step size Δ (Figure 2.6). Clearly, the distance between X and $\hat{X}$ is bounded as $Q = |X - \hat{X}| \leq \frac{\Delta}{2}$. The encoder will communicate $\hat{X}$ to the decoder, which is within the distortion requirement. Note that the distance between $\hat{X}$ and Y is bounded by

$$|\hat{X} - Y| \leq |\hat{X} - X| + |X - Y| < \frac{\Delta}{2} + \frac{3\Delta}{2} = 2\Delta.$$

Since the decoder has access to Y, it knows that $\hat{X}$ must be one of the four codewords that are within $\pm 2\Delta$ from Y. Had the encoder also had access to Y, it could have indicated with two bits which one of these four codewords $\hat{X}$ is. However,

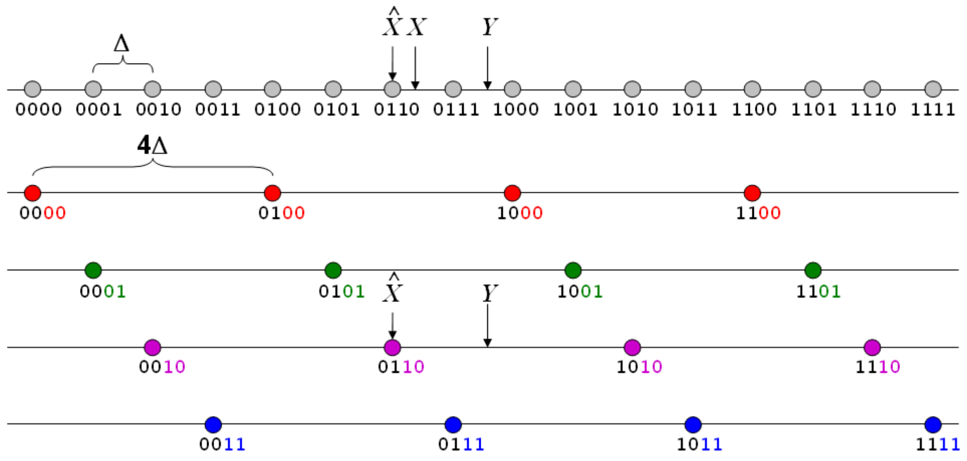

Figure 2.6: X is a scalar real-valued number that the encoder is trying to communicate to the decoder within distortion $\pm\frac{\Delta}{2}$. The decoder has access to side information Y. Y is a noisy version of X, and can be expressed as $Y = X + N$ where N is the correlation noise. It is known that X and Y are correlated such that $|Y - X| < \frac{3\Delta}{2}$. We can think of the quantizer as consisting of four interleaved quantizers (cosets), each containing codewords whose binary labels end with the same two least significant bits. The encoder, after quantizing X to $\hat{X}$, will indicate to the decoder which one of these interleaved quantizers $\hat{X}$ belongs to. In this case, it is the quantizer in which all the codewords' binary labels end with "10". The decoder can declare the closest codeword to Y in the indicated interleaved quantizer as $\hat{X}$.

even when the encoder does not have access to Y, it is possible to communicate $\hat{X}$ to the decoder using only two bits. To see this, we can think of the quantizer (codebook) as consisting of four interleaved quantizers (cosets), each of step size 4Δ, as shown in Figure 2.6. The encoder, after quantizing X to $\hat{X}$, can indicate to the decoder which one of these interleaved quantizers (coset) $\hat{X}$ belongs to, which also requires two bits. Since the step size of each of the four interleaved quantizers is 4Δ, each of them has exactly one of the four codewords that are within $\pm 2\Delta$ from Y. Therefore, the decoder can declare the closest codeword to Y in the indicated interleaved quantizer as $\hat{X}$.

In assigning a unique two-bit symbol, or syndrome, to each interleaved quantizer (coset), we see that each of them contains codewords whose binary labels share the same two least significant bits. For example, the labels of the codewords in the first coset all end with bits "00". Therefore a natural way to indicate a coset is to use the common least significant bits. The number of least significant bits needed to indicate a coset depends on how many cosets the codebook is broken into, which in turn depends on the statistics of the correlation noise N. We adopt this multi-level coding scheme [45] in our implementation.

Like in the lossless coding example, even if Y at the decoder becomes corrupted, as long as it does not violate the correlation constraint, i.e. as long as $Y - \hat{X} < 2\Delta$, decoding will succeed. In general, the fact that the encoder is able to compress the source X^n using only the *statistical* correlation between X^n and Y^n, without having access to a *deterministic* copy of the side-information Y^n, is the reason for the inherent robustness of the distributed source coding framework and makes it a promising framework to enables robust video transmission.

Let us now take a more formal look at Wyner-Ziv encoding and decoding.

Wyner-Ziv encoding and decoding: As in regular source coding, encoding proceeds by first designing a rate-distortion codebook of rate R' (containing $2^{nR'}$ codewords) constituting the space of quantized codewords for X. Each n-length block of source samples $\mathbf{X}$ is first quantized to the "nearest" codeword in the codebook. As in the illustrative example above, the quantized codeword space (of size $2^{nR'}$ codewords) is further partitioned into 2^{nR} cosets or bins ($R < R'$) so that each bin contains $2^{n(R'-R)}$ codewords. This can be achieved by the information theoretic operation of random binning. The encoder transmits only the index of the bin in which the quantized codeword lies and thereby only needs R bits/sample.

The decoder receives the bin index and disambiguates the correct codeword in this bin by exploiting the correlation between the codeword and the matching n-length block of side-information samples $\mathbf{Y}$. This operation is akin to channel decoding. Once the decoder recovers the codeword, if MSE is the distortion measure, it forms the minimum MSE estimate of the source to achieve an MSE of D.

An important feature of the coset binning method that we exploit is the fact that if the side information at the decoder is inferior to what the DSC code was designed for, the decoder can still make use of this transmission if a small amount of additional information is made available. Continuing the example above, suppose that after the transmission, the encoder finds out that the actual side information Y' available at the decoder is of an inferior quality $|Y' - X| < \frac{7\Delta}{2}$. All the encoder needs to do is to further partition each of the four interleaved quantizers into two sub-quantizers and indicate to the decoder which sub-quantizer $\hat{X}$ belongs to using one additional bit. Together with the two bit originally received, the decoder can

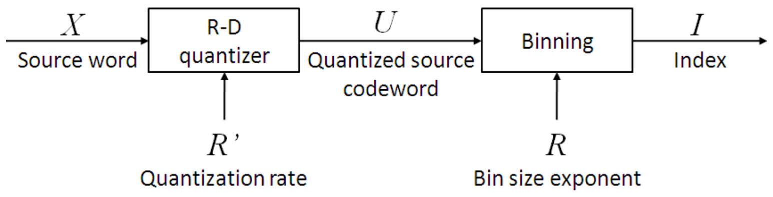

(a)

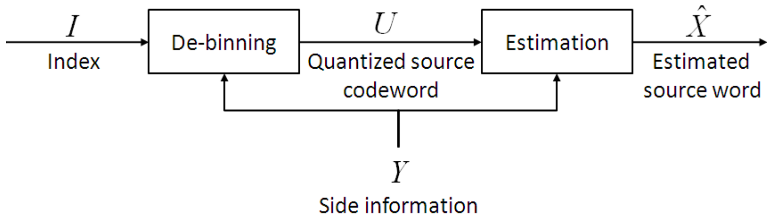

(b)

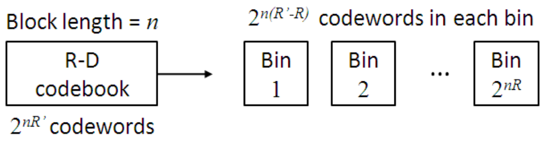

(c)

Figure 2.7: (a) Structure of distributed encoders: encoding consists of quantization followed by a binning operation. (b) Structure of distributed decoders: decoding consists of de-binning followed by estimation. (c) Structure of the codebook bins: the R–D codebook containing approximately $2^{nR'}$ codewords is partitioned into 2^{nR} bins each with approximately $2^{n(R'-R)}$ codewords.

now correctly decode $\hat{X}$ given the inferior side information Y'. It is important to note that the two bits sent in the first transmission are entirely useful even given the inferior side information. This feature is unique to the DSC framework, which allows us to take a layered approach and separate the baseline layer and robustness layer without losing any compression efficiency. This separation will further enable compression of the robustness layer as we will later demonstrate.

From distributed source coding principles to video coding

There are two major assumptions in the classical distributed source coding setup. First, the decoder has one and only one side information to use. Second, both the encoder and decoder know the correlation between the source and the side information. These assumptions are unfortunately not true for practical video coding. First, video data is highly redundant both spatially and temporally. For each block, there are a lot of correlated previously decoded blocks available at the decoder that can be used as the side information. When there are transmission packet drops, it becomes unclear which previously decoded block is the most correlated to the current block. Second, neither the encoder nor the decoder has knowledge of the correlation between the source and side information because video data is highly non-stationary. Even though the encoder can learn the correlation through motion search, in the presence of packet drops that the encoder cannot anticipate, correlation estimation becomes very challenging.

These differences between theory and practice dictates that there are two important aspect to video coding using distributed principles. First, the decoder needs to use a high-quality side information. If the decoder picks a side information that is poorly correlated to the source, the encoding rate will be higher than necessary to ensure successful decoding, thus losing compression efficiency. Second, the encoder needs to be able to accurately estimate the correlation between the current block and the side information. If we underestimate the correlation between the current block and the best predictor block at the decoder, we will use a channel code that is stronger than necessary, hence losing compression efficiency. On the other hand, if we overestimate the correlation, channel decoding will fail, causing video quality degradation.

In the following chapter, we will illustrate through a simple illustrative example how the proposed system addresses these two issues simultaneously by making use of channel characteristics and decoder's knowledge regarding past packet drop patterns.

Chapter 3

Distributed source coding based robust video transmission over networks with bursty losses

3.1 Related work

There have been a number of novel and interesting works that use distributed source coding to tackle various challenges in video coding and transmission. The challenges include but are not limited to low-complexity video encoding (e.g. [21, 37, 7] and the references within), robust video transmission (e.g. [37, 40, 21, 27]), scalable video coding (e.g. [51, 46]), and multi-view video coding (e.g. [23] and the references within). In this section, we focus on reviewing related works on robust video transmission using DSC [37, 40, 21, 47, 27], and flexible video decoding using DSC [12].

3.1.1 Robust video transmission using distributed source coding

In the example in Section 2.1.3, we note that as long as the side information Y remains within $\pm\frac{3\Delta}{2}$ of X, the decoder will always correctly decode $\hat{X}$. This flexibility plays an important role in enabling robust video transmission. In a nutshell, in the face of transmission packet loss, the encoder cannot have access to the decoder's reconstruction of previously received frames. However, if the encoder can accurately estimate the correlation between the current frame and the decoder reconstruction of the previous frame(s) and encode the current frame accordingly, decoding will succeed with high probability. This benefit can be realized in two ways:

1. overhaul the predictive coding framework and build an entirely DSC-based video codec [37] that is inherently robust; or

2. enhance the robustness of MPEG/H.26x transmission by sending DSC-coded data alongside predictively encoded video bitstream [40, 21, 47, 27] to correct drift.

In [37], each block is classified into one of the 16 modes based on the mean square error between the current block and the co-located block in the previous frame. The mode of the block indicates the statistical correlation between this block and the best predictor block available at the decoder, even though the encoder has no access to the best predictor block. This coding architecture enables very low-complexity encoding as the encoder eliminates the computationally expensive motion search. However, being constrained to such low encoding complexity makes it extremely difficult to accurately estimate the correlation between the current block and the best predictor block available at the decoder, because video data is highly non-stationary. As a result, the mode of each block is typically an underestimation of the correlation and thus allocates more rate for each block than necessary. While this underestimate has the benefit of excellent robustness performance (as many blocks can lead to successful decoding), the compression efficiency is suboptimal when where are no transmission losses. Further, the compression level is not tailored to any specific channel condition.

In this work, we allow the encoder to do motion search and instead explore the role of motion search at the encoder in enabling robust video transmission. While it is clear that motion search can lead to excellent compression efficiency as shown by predictive coding, we will show that it can be a very useful tool in robust video coding that can tailor to specific channel conditions.

In [40, 21, 47, 27], the authors send extra distributed source coded data alongside a baseline predictively coded bitstream. They differ in how frequently DSC-data is sent, how the correlation is estimated, and what is used as the source and side information.

Specifically, in [40], the authors periodically mark some of the P-frames as "peg" frames. At each peg frame, distributed source coded information is used for the decoder to correct for the accumulated errors up to the peg frame. In [21], the input to the Wyner-Ziv encoder is the predictively encoded bitstream itself, i.e. the residual signal of the video, but using a coarser quantization. At the decoder, the baseline reconstructed video is re-encoded and with coarser quantization. This coarsely re-encoded bitstream is used as side information for the Wyner-Ziv decoding. [27] extends this framework to include unequal error protection on the motion vectors to achieve better performance. In [47], the authors proposes an analytically tractable recursive algorithm that dynamically tracks the correlation between the source (current block) and the side information (decoder reconstructed current block) and sends DSC-coded data for every frame.

The proposed work share similarity to [40, 21, 47, 27] in that we also take a layered approach. The compressed bitstream of the proposed system also consists of two parts, the baseline layer and the robustness layer. The baseline layer suffices to recover the video when there are no packet drops. The robustness layer is used to correct for drift. However, the baseline layer in the proposed work consists of DSC-coded data instead of MPEG-style predictively coded data. The correlation estimation algorithm used to determine the encoding rate of the robustness layer is also completely different. We will see in Section 3.3 why it is beneficial to have a DSC-coded baseline layer and why the proposed rate allocation scheme is suitable for transmission channels with bursty packet drops.

3.1.2 Flexible video decoding using distributed source coding

In some cases, the encoder has "partial" knowledge of the decoder side information. Consider the setup in Figure 3.1. X^n is a length-n i.i.d. source sequence. A set of P possible side information realizations $\{Y_i^n\}_{i=1}^P$ are available at the encoder. However, only one side information realization, Y_k^n is available at the decoder. The joint distributions $p_{X,Y_i}(x, y_i)$, $i \in \{1, \dots, P\}$ are known at both the encoder and the decoder. But only the decoder knows the identity k of the side information realization. The goal is to recover X^n exactly. Since the encoder has no knowledge about which one of the side information will be realized at the decoder, predictive coding does not work. On the other hand, using distributed source coding, we can design the channel code according to the least correlated side information, and achieve much better result than encoding X^n independently. It was shown in [18] that for the lossless coding case, Slepian-Wolf coding at rate $R = \max_i H(X|Y_i)$ is asymptotically optimal for this setup.

This setup appears in some interesting multimedia applications. In a multiple-camera setup, X^n can be thought of as the current frame of a target camera. $\{Y_i^n\}_{i=1}^P$ are the previous frames from all the cameras. Using a distributed source coding framework, we can decode the current frame X^n using the previous frame from any camera, allowing instant camera view switching [12]. In a single-camera setup with $P = 2$, X^n can be thought of as Frame t. Y_1^n is Frame $t - 1$, and Y_2^n is Frame $t + 1$. Encoding X^n according to the less correlated between Y_1^n and Y_2^n will allow Frame t to be decodable from either Frame $t - 1$ or $t + 1$, thereby enabling quick video rewind [12].

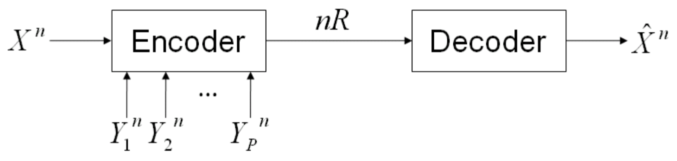

Figure 3.1: Flexible decoding setup: X^n is a length-n i.i.d. source sequence. A set of P possible side information realizations $\{Y_i^n\}_{i=1}^P$ are available at the encoder. Only one side information realization, Y_k^n is available at the decoder. The joint distributions $p_{X,Y_i}(x, y_i)$, $i \in \{1, \ldots, P\}$ are known at both the encoder and the decoder. But only the decoder knows the identity k of the side information realization. The goal is to decode X^n within some distortion constraint.

Our work shares the philosophy of associating each encoding block with multiple predictor blocks, i.e. multiple side information, and aim to decode successfully as long as at least one of the predictors is available at the decoder. As an example, in our setup, X^n can be thought of as the current block to be encoded. Y_1^n is the best predictor among all the blocks in previous frames. Y_2^n is the best predictor two frames ago, and so on. We aim to decode correctly as long as at least one of the P best predictors has been correctly reconstructed at the decoder. Using the approach in [18] or [12], one needs to encode X^n according to the least correlated side information. However, our approach take advantage of the important fact that even though the best predictor Y_1^n may not always be available at the decoder, it is available at the decoder most of the time. Further, since the decoder has knowledge regarding past channel transmission errors, it can make intelligent decisions regarding which predictor to use. This allows us to achieve significant rate reduction. We will explain how this can be done in detail in the following section.

3.2 Illustrative example

In this section, we use an illustrative example to demonstrate the intuition behind the system design.

We consider the following simplified source model for motion compensated video. The frame at time t is made up of n non-overlapping blocks $\vec{X}_i(t),\ i = 1, 2, \ldots, n$. Each of of the blocks is a vector of length L (assumed to be large here), whose elements belong to a finite field. Each of these blocks can be conceptualized as a transmission packet containing one or many encoding blocks. The elements are transform coefficients of the encoding block(s). We make the simplifying assumption that the motion compensated predictors are also non-overlapping. Thus, as shown in Figure 3.2, the time evolution of these blocks can be modeled by writing the block $\vec{X}_i(t)$ as $\vec{X}_i(t) = \vec{X}_i(t-1) + \vec{Z}_i(t)$. In other words, each block is the sum

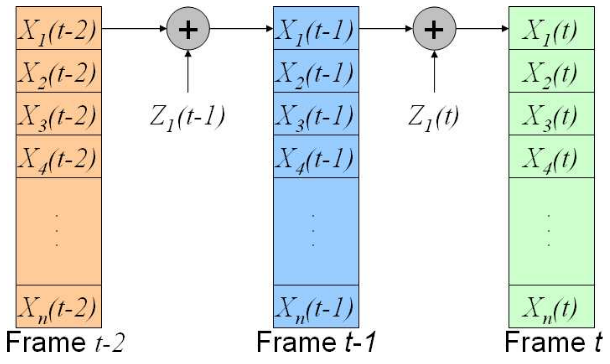

Figure 3.2: Simplified source model for motion compensated video. The frame at time t is made up of n non-overlapping blocks $\vec{X}_i(t)$, $i = 1, 2, \ldots, n$ each of which is a vector of length L (assumed to be large here), and whose elements belong to a finite field. The time evolution of these blocks is modeled by writing the block $\vec{X}_i(t)$ as $\vec{X}_i(t) = \vec{X}_i(t-1) + \vec{Z}_i(t)$, where $\vec{Z}_i(t)$ represents an innovation process that is i.i.d. over i and t.

of the motion-compensated predictor block $\vec{X}_i(t-1)$ from the previous frame and an innovation process $\vec{Z}_i(t)$ which is independent and identically distributed (i.i.d.) over i and t. Also, the elements of $\vec{Z}_i(t)$ are i.i.d. random variables according to a distribution p_Z with entropy per coefficient $H(Z)$.

In a motion-compensated predictive coding framework, the innovation, or residual signal, $\vec{Z}_i(t)$ is entropy-coded and sent[1] at time t. This requires a rate of $H(Z)$ per coefficient. Upon receiving this, the decoder can recover $\vec{X}_i(t)$ if it has access to side information $\vec{X}_i(t-1)$. Alternatively, one could use the concet of distributed source coding, specifically Slepian-Wolf coding [43], to achieve the same effect. Here the space of all possible $\vec{X}_i(t)$ sequences is partitioned into $2^{H(\vec{X}_i(t)|\vec{X}_i(t-1))}$ cosets and the index of the coset to which $\vec{X}_i(t)$ belongs is sent. This also requires a

[1]In practice the innovation is quantized, but under our finite field model for the source, we assume that the quantization has already been performed to a desired fidelity. Hence we will require that the whole vector $\vec{X}_i(t)$ be recovered at the decoder.

rate of $H(\vec{X}_i(t)|\vec{X}_i(t-1))/L = H(Z)$. It can be shown that with high probability, the decoder will be able to successfully disambiguate $\vec{X}_i(t)$ from the coset indicated, provided it has access to $\vec{X}_i(t-1)$. Thus, asymptotically in L, both the systems operate at the same rate $H(Z)$. The key difference between the systems is that the information sent to the decoder by the DSC-based system depends directly on the current block $\vec{X}_i(t)$, whereas the MCPC-based system sends information which depends on both the predictor and the current block. Note that in the absence of packet drops, under the simplified model, both the predictive coding framework and the DSC framework require the same rate $H(Z)$ per coefficient. In practice, video coding is a lossy coding process. Theoretically, Wyner-Ziv coding (lossy source coding with decoder side information) suffers from a small amount of rate loss [52] compared to the conventional predictive lossy source coding unless the innovation is Gaussian. But the compression performance of the two systems are still comparable as shown in Section 3.4.

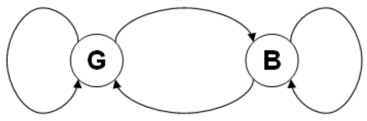

Figure 3.3: To represent the bursty nature of lossy wireless channels, we adopt a two-state model to capture the effect of bursty packet drops on the video frames. If a frame is hit by a burst of packet drops, e.g. due to a fade in cellular network, we say the frame is in a "bad" state. Otherwise, it is considered to be in a "good" state. The state evolves at every time step according to a probability transition matrix. In the "good" state, the channel erases packets with probability p_g. In the "bad" state, the channel erases packets with probability p_b. It is assumed that $p_b \gg p_g$.

We adopt a two-state frame state model to capture the effect of bursty channel losses on video frames. If a frame is hit by a burst of packet drops, e.g. due to a wireless channel fade, we say the frame is in a "*bad*" state[2]. Otherwise, the frame is considered to be in a "*good*" state. Note that we are modeling the effect of the channel on the video frames, not the channel itself. The state evolves at every time step according to a probability transition matrix (Figure 3.3). At each time t, both the MCPC and DSC-based systems will send n packets, one for each block in Frame t. In addition, both systems will send some extra packets to combat the effects of the channel, as described later. The channel erases packets in Frame t independently with probability p_g if the frame is in the "good" state and with probability p_b if the frame is in a "bad" state.[3] We assume $p_g \ll p_b$. We model the latency constraint of the system by requiring the decoder to reproduce Frame t upon receiving the blocks sent at time t. From now on, we will assume knowledge of p_g and p_b. In practice, this can be done with the help of a slow and low-rate feedback channel. This is not the same as assuming knowledge of which state each transmitted frame is in, which would require an almost instantaneous feedback.

Let us first consider the approach of protecting an MCPC-coded bitstream with FEC codes. At time t, it will send parity packets on the residual signals $\vec{Z}_i(t)$. Due to the nature of predictively compressed data, to decode Frame t correctly, we need to have successfully recovered the residual signals of all the previous frames. This requires that the residual signals of each frame be successfully transmitted regardless of the frame state. The delay constraint requires the FEC code be designed targeting the worst possible channel condition, i.e. the "bad" frame state. For a large

[2]The duration of a wireless channel fade is typically considered to be of the order of 5 ms, which is much shorter than the transmission time of an entire video frame. Thus we do not model the case in which a burst of packet drops spans two frames in this example.

[3]Though physical packet drops are not independent when the frame is in a bad state, we can obtain independent block drop patterns through interleaving.

n, the rate required is at least

$$R_{\text{FEC}} = \frac{H(Z)}{1-p_b}. \tag{3.1}$$

This can be achieved by using maximum distance separable (MDS) codes, such as the Reed-Solomon codes, as reviewed in Section 2.1.2.

The proposed DSC-based system takes a different approach in handling packet drops. When the syndrome for a block is lost in a "bad" frame due to a channel erasure, the decoder will not attempt to decode that block, but tries to arrest the effects of such losses on future frames. Suppose Frame $t-1$ is in the "bad" state but Frame $t-2$ is entirely correctly reconstructed. Obviously, the predictor blocks for some of the current blocks will be in error due to packet losses at time $t-1$. Let $\vec{X}_i(t)$ be one such block. The proposed DSC-based system tries to use the next best predictor $\vec{X}_i(t-2)$ from two frames ago as side information. However, $\vec{X}_i(t-2)$ is of an inferior quality to $\vec{X}_i(t-1)$. In order to successfully decode, the decoder now requires the number of cosets to be $2^{H(\vec{X}_i(t)|\vec{X}_i(t-2))}$ instead of the original $2^{H(\vec{X}_i(t)|\vec{X}_i(t-1))} = 2^{LH(Z)}$. As reviewed in Section 2.1.3, this can be achieved by further partitioning each of the original $2^{LH(Z)}$ cosets into $2^{L(H(Z*Z)-H(Z))}$ sub-cosets. Here we defined $Z*Z$ as the sum of two i.i.d. random variables with marginal distributions p_Z such that $H(\vec{X}_i(t)|\vec{X}_i(t-2)) = H(Z*Z)$. In addition to the coset information at rate $H(Z)$, incremental syndrome to indicate the sub-coset at rate $H(Z*Z)-H(Z)$ is also required to be sent by the encoder. This is analogous to the additional bit needed to decode from the inferior side information in the example in

Section 2.1.3. Thus, the rate needed by the DSC-based system is now

$$R = \frac{H(Z * Z)}{1 - p_g} \tag{3.2}$$

$$= \frac{H(Z)}{1 - p_g} + \frac{H(Z * Z) - H(Z)}{1 - p_g}. \tag{3.3}$$

The factor $\frac{1}{1-p_g}$ comes from the extra rate needed by an MDS code to protect these coset indices against packet drops in a "good" frame state. The first term in (3.3) is the bare minimum needed to ensure successful decoding if the frames are always in the "good" state. The second term is the incremental information needed to combat a burst of packet drops in Frame $t-1$. If the encoder adopts this scheme, then clearly the decoder can recover block $\vec{X}_i(t)$ if either $\vec{X}_i(t-1)$ or $\vec{X}_i(t-2)$ is sent. This is very similar to the flexible decoding technique proposed in [12] in spirit. However, we can improve upon this scheme by taking advantage of the fact that not all blocks in Frame $t-1$ are lost during transmission and not all blocks in Frame t need additional syndrome to decode correctly.

Since only p_b fraction of the blocks in Frame $t-1$ are erroneously reconstructed, only p_b fraction of the blocks in Frame t will be decoded using predictors in Frame $t-2$ thereby needing incremental syndromes to be correctly decoded. The other $1-p_b$ fraction of the blocks, whose predictors are not lost in Frame $t-1$, can be correctly decoded. Further, once they are correctly decoded, the incremental syndromes for these blocks can be inferred. Therefore, even when no incremental syndromes are sent, the decoder is able to recover $1-p_b$ fraction of these sub-coset indices. Since the decoder also has knowledge of the location of the corrupted blocks, it is as if the incremental syndromes went through an erasure channel with erasure probability p_b. This allows the encoder to send the incremental syndromes at a reduced rate by applying an erasure code over the sub-coset indices for all blocks in Frame t and sending only the parity at rate $p_b(H(Z*Z)-H(Z))$. The total rate needed can therefore be reduced to

$$R_{\text{DSC}} = \frac{H(Z)}{1-p_g} + \frac{p_b(H(Z*Z)-H(Z))}{1-p_g}. \tag{3.4}$$

The rate difference between the pure FEC-based approach and the proposed DSC-based approach is

$$\begin{aligned} \Delta R &= R_{\text{FEC}} - R_{\text{DSC}} && (3.5)\\ &= \frac{p_b(2H(Z)-H(Z*Z))}{1-p_g} + \frac{(p_b^2-p_g)H(Z)}{(1-p_b)(1-p_g)}. && (3.6) \end{aligned}$$

Since $H(Z*Z) \leq 2H(Z)$, the difference is guaranteed to be positive for $p_g < p_b^2$. Using the proposed DSC-based strategy, the analysis holds as long as no two consecutive frames are both in the "bad" state.

The philosophy behind the illustrative example can be easily extended to the case where more than one frames can be hit by bursts of packet drops consecutively. One solution is for each block to have more than two predictors and aim to decode correctly as long as one of the predictors has been reconstructed correctly at the decoder. For example, suppose at most two frames can be in the "bad" state consecutively, the rate at which the encoder needs to operate is

$$R_{\text{DSC}} = \frac{H(Z)}{1-p_g} + \frac{p_b(H(Z*Z)-H(Z))}{1-p_g} + \frac{p_b^2(H(Z*Z*Z)-H(Z*Z))}{1-p_g}. \tag{3.7}$$

Compared to (3.4), (3.7) has an additional third term, which is used to decode the current block using the predictor in Frame $t-3$ if both the predictor in Frame $t-1$ and the one in Frame $t-2$ have been corrupted due to packet drops.

Clearly, as we increase the number of consecutive "bad" frames that the system is designed to tolerate, the gain of the proposed approach decreases compared to the FEC approach. In practice, we have to design for a certain *outage* probability. An outage is defined as the event in which the number of consecutive "bad" frames goes beyond what the encoder is designed for. From the real-world channel simulator we obtained for the CDMA 2000 1x cellular network, we find it sufficient to associate each block with only two predictors, as detailed in Section 3.4.

It is clear from this example that the proposed scheme is not always advantageous compared to the predictive coding scheme. First, if the channel does not have a bursty nature, i.e. p_g and p_b are close, there is not necessarily a rate gain. Second, we need the second predictor to be reasonably correlated to the current block, i.e. we would like $H(Z * Z) - H(Z)$ to be small. The strong and typically persistent temporal correlation unique to video data makes this possible.

Finite block length analysis: The rough argument above assumed a large number of packets n in each frame. This is not true for practical video transmission. While the philosophy we presented in the illustrative example holds regardless of the block length, the specific parameters for a practical system need to be adjusted taking the block length n into consideration.

For example, suppose we want to use an erasure code to target erasure probability p. The infinite block length analysis would suggest that we need an overhead of $\frac{np}{1-p}$ redundant packets such that all the packets can be recovered with probability close to 1. However, this is not the case when n is small. In an extreme example, suppose there are only 2 packets in a frame and the erasure probability is 0.5. We would transmit 2 redundant parity packets as prescribed by the infinite block length analysis. With probability $\frac{1}{16}$, all four packets will be lost. With probability $\frac{1}{4}$, three out of four packets will be lost. In either case, there will be unrecoverable packet drops. In fact, we need to send 8 redundant packets to ensure all the data packets can be recovered with probability 0.99. The effect of finite block length will affect both the choice of FEC used to guarantee packet delivery in a "good" frame and the rebate factor we can get for the robustness layer.

Here, we use a more exact analysis of the dynamics for a small number of packets n per frame. With a small n, both the FEC rate to use in a good frame state and the rebate factor p_b that we observe in the previous analysis are overly optimistic for practical scenarios. This analysis will provide us with a guideline on how to numerically obtain an appropriate set of parameters given fixed n, p_g, and p_b. This finite block length analysis will also demonstrate the disadvantage of the FEC-based approach when the delay constraint is stringent and FEC codes can be applied only to a small number of blocks at a time.

All the codes are assumed to be be MDS. We compute the marginal probability of error in reproducing a packet at the decoder for a particular set of parameters. This probability is conditional on the frame state sequence. Specifically, $X_i(t)$ will be in error if any of the following events happens:

- The packet containing $X_i(t)$ is lost;
- The packet containing $X_i(t)$ is received but both $X_i(t-1)$ and $X_i(t-2)$ are in error;
- The packet containing $X_i(t)$ is received, $X_i(t-1)$ is erroneous, $X_i(t-2)$ is correct but the robustness layer for time $t-1$ is not decodable, i.e. more

predictors are corrupted in Frame $t-1$ than expected.

Using this, the probability of $X_i(t)$ being in error can be recursively evaluated for each frame state sequence. We can choose the parameters, namely the FEC overhead in a "good" state and the rebate factor of the robustness layer, using any desired criteria. For example, we can set a bound for the average probability of $X_i(t)$ being in error over a large number of state sequences. Though there is not a closed form solution for the parameters as a function of the target error event probability, we can numerically solve for them given a fixed block length n, p_g, and p_b. Note that the decisions for the FEC overhead in a "good" state and the rebate factor of the robustness layer are interdependent. Among all solutions that achieve the same error event probability, we choose the one that is the most rate efficient.

Now we use an example to compare the performance of the proposed system to the one in which predictively coded data is protected with MDS FEC. We compute and compare the probability of the decoder failing to recover a video block as a function of time under a typical channel state sequence. We choose our parameters to closely match the simulation setup presented in Section 3.4 to get a sense of the expected performance. Based on the practical error masks used in the Section 3.4, we set $p_g = 0.03$, $p_b = 0.3$. The frame state is "bad" at times $t = 6, 17, 38$, and "good" at other times. We choose $n = 30$ which is a realistic value for the packets per frame. We assume a binary field with a Bernoulli innovation process Z, i.e.

$$\Pr(Z = 1) = 1 - \Pr(Z = 0) = p.$$

We use $p = 0.11$, which corresponds to a rate of $H(Z) = 0.5$ and $H(Z * Z) = 0.71$.

The long block length analysis would suggests $p_b(H(Z*Z) - H(Z)) = 0.063$ bit/symbol for the sub-coset indices, which is 12.6% of the baseline coset indices.

Here, we choose the rate for the sub-coset indices to be 26% of the baseline information instead to target a certain block recovery probability. For comparison, we consider two conventional predictive coding systems which use MDS FEC: one operates at the same overall rate as the DSC-based system by using 26% extra rate for FEC, and the other uses 70% extra rate for FEC. Figure 3.4 shows that the proposed system has a high block recovery failure rate for frames in a “bad” state, but can immediately improve performance in the following “good” state. In fact, under the same latency constraint, to deliver similar performance under “good” frame state as the proposed DSC-based system, an MCPC-based system protected with MDS FEC needs 70% extra rate for the FEC. This difference is even bigger when the block length n becomes smaller.

3.3 System implementation

We implement a practical DSC-based video coder built upon the intuition from the illustrative example. Just like in the illustrative example, each encoding block is associated with two predictors. We design to successfully decode as long as at least one of these predictors is correctly reconstructed at the decoder. The compressed bitstream consists of a baseline layer and a robustness layer. The baseline layer contains syndromes to reconstruct each block using the best predictor. It suffices to reconstruct the entire video perfectly when the compressed bitstream is transmitted without error. The robustness layer contains additional incremental syndromes. When combined with the baseline syndrome, these robustness syndromes can decode blocks using the second best predictors, as long as the fraction of blocks whose best predictors are not available is within a designed threshold. We now detail

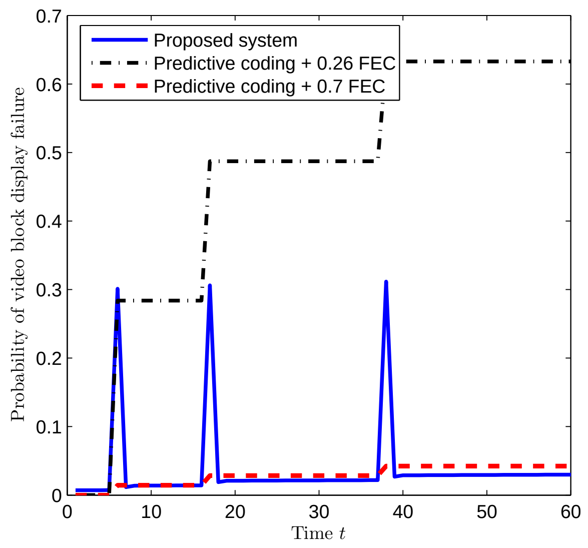

Figure 3.4: Finite block length analysis for the illustrative example: The plot shows the probability of the decoder failing to recover a video block as a function of time under a typical frame state sequence. The frame state is "bad" at times $t = 6, 17, 38$, and "good" at other times. We set $p_b = 0.3$ and $p_g = 0.03$. We assume a binary field with a Bernoulli innovation process Z and factor $p = 0.11$. The number of packets in each frame is $n = 30$ for practical considerations. The rate for the sub-coset information is chosen to be 26% of the rate used for the baseline coset information. For comparison, we consider two MCPC-based systems with FEC: one operates at the same overall rate as the DSC-based system by using 26% extra rate for FEC, and the other uses 70% extra rate for FEC. We assume MDS codes for all systems. Under the same latency constraint, to deliver similar performance under "good" frame state as the proposed DSC-based system, which uses 26% extra rate for sub-coset information, an MCPC-based system needs 70% extra rate for the FEC.

the implementation of the encoder and decoder respectively.

3.3.1 Encoder

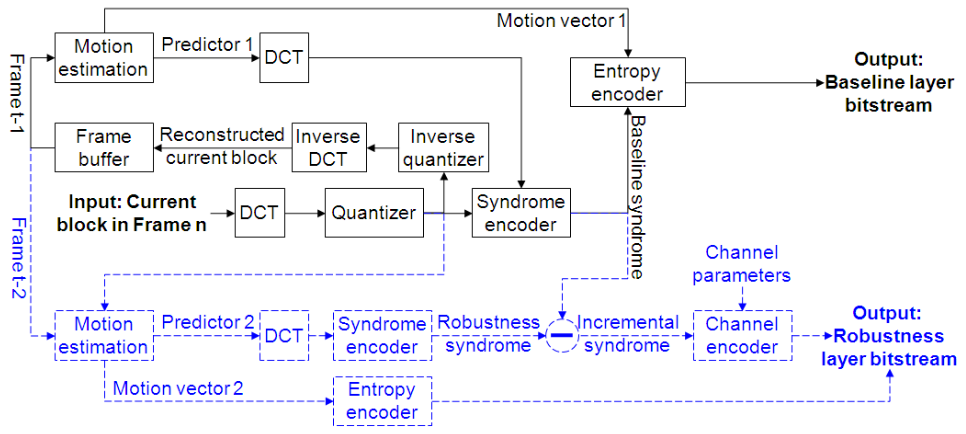

Figure 3.5: Block diagram for the encoder. Components in solid black lines belong to the baseline layer while components in dashed blue lines belong to the robustness layer.

The block diagram for the encoder is depicted in Figure 3.5. Components in solid black lines belong to the baseline layer whereas components in dashed blue lines belong to the robustness layer.

Baseline layer

Video frames are identified by independently-coded frames (I-frames) and DSC-coded frames (WZ-frames). Each I-frame can be followed by as many WZ-frames as desired. I-frames are encoded just like in H.263+. For WZ-frames, the video frame to be encoded is divided into non-overlapping spatial blocks. We use blocks of size 8×8 in our current implementation. Each block can be skipped, intra-coded, or syndrome-coded. To make this mode decision, motion estimation in the pixel domain is carried out to locate the best predictor in the reconstructed reference frame. The mean square error between the current block and the best predictor will determine whether the block will be skipped, intra-coded or syndrome-coded. Skip and intra blocks are encoded the same way as in H.263+. To syndrome-code the i^{th} block in the t^{th} frame, the following steps are followed.

- **DCT:** Take DCT of both the current block and the best predictor block. We denote the non-quantized DCT coefficients of the current block and its motion-compensated predictor by $\{X_i^j(t)\}_{j=1}^{64}$ and $\{X_i^{j'}(t-1)\}_{j=1}^{64}$, respectively.
- **Quantization:** Quantize the DCT coefficients of the current block $\{X_i^j(t)\}_{j=1}^{64}$ to $\{\hat{X}_i^j(t)\}_{j=1}^{64}$ using a scalar quantizer.
- **Syndrome coding:** Generate syndrome for $\{\hat{X}_i^j(t)\}_{j=1}^{64}$ using the multi-level coding scheme [45] as described in Section 2.1.3. Recall that for each DCT coefficient, its syndrome consists of the least significant bits of its binary representation that cannot be inferred from the side information. For the j^{th} coefficient of this block, the number of least significant bits of the binary representation of $\hat{X}_i^j(t)$ that need to be sent can be computed as

$$L_i^j(t-1) = \max\left(0, \left\lceil \log_2 \frac{\left|\hat{X}_i^j(t) - X_i^{j'}(t-1)\right|}{\Delta} \right\rceil + 1\right),$$

where Δ is the quantization step size determined by the desired video quality. For example, let the DC coefficient of the i^{th} block in the t^{th} frame be 156. Let the quantization step size be 10. Therefore $\hat{X}_i^1(t) = 160$, whose label is 16 in decimal and 10000 in binary. Let the DC coefficient of the motion-compensated predictor for this block in Frame $t-1$ be 142. The number of bit planes needed is therefore 2 and these bits are “00”. Theoretically, the correlation between the source and the side information is known at both the encoder and the decoder. Thus both the encoder and the decoder would know that two bits need to be sent for this coefficient. However, this is not the case in practice. The encoder needs to indicate to the decoder both the number of bit planes to send, which essentially describes the correlation statistics, and what those bits are. We use a standard variable length coding technique to map this information to a unique symbol.

- **Entropy coding:** The symbols of all the DCT coefficients' syndromes within a block are zig-zag scanned, run-length coded and then arithmetic coded (summarized as Entropy Coding in the block diagram). The motion vectors within each slice are differentially coded just like in H.26x[4].

- **FEC coding:** Finally, an MDS FEC code is applied to the base layer to combat packet drops when the frame is in the “good” state. If the “good” state packet drop rate is sufficiently low, this layer of protection is optional.

- **Reconstruction:** Inverse quantization, inverse DCT and estimation is carried out to generate the encoder reconstruction of the current block, which is in turn written back to frame memory.

The resulting compressed bitstream corresponds to the first term in (3.4). This is the bare minimum rate needed when the frames are in the “good” state all the time.

[4]We preserve independent decodability of a slice.

Robustness layer

The robustness layer needs to identify a second predictor and then encode the sub-coset indices, or incremental syndromes, such that decoding will succeed as long as one of the two predictors are corrected decoded. Motion compensation in the pixel domain is carried out to locate a secondary predictor in the reconstructed Frame $(t-2)$. To reduce search complexity, we center the search around the interpolated best motion vector obtained in the baseline layer encoding, and limit the search range to ± 2 pixels with half-pixel accuracy. We denote the non-quantized DCT transform of the second 8×8 predictor by $\{X_i^{j''}(t-2)\}_{j=1}^{64}$. $\{X_i^{j''}(t-2)\}_{j=1}^{64}$ is typically a partially degraded side information for $\{X_i^j(t)\}_{j=1}^{64}$ compared to $\{X_i^{j'}(t-1)\}_{j=1}^{64}$. To correctly decode $\hat{X}_i^j(t)$ using $\hat{X}_i^{j''}(t-2)$ as side information, the decoder needs to know $L_i^j(t-2) = \max\left(0, \left\lceil \log_2 \frac{\left|\hat{X}_i^j(t) - X_i^{j''}(t-2)\right|}{\Delta} \right\rceil + 1\right)$ least significant bits of $\hat{X}_i^j(t)$. If $L_i^{j''}(t-2) > L_i^j(t-1)$, incremental syndrome needs to be sent in the robustness layer. We now detail the implementation.

If we try to decode $\{\hat{X}_i^j(t)\}_{j=1}^{64}$ using only the baseline syndromes and $\{X_i^{j''}(t-2)\}_{j=1}^{64}$ as side information, typically the result will be at least partially erroneous. To correct for the errors with the robustness layer, we take the bit plane coding approach and apply low density parity check (LDPC) codes of different rates on different bit planes of the quantized DCT coefficients across the current frame except for intra and skip blocks.

Figure 3.6(a) shows the bit plane representation of the DC and first seven AC DCT coefficients of a block. The bits marked as black are the ones that have already been sent in the base layer. Let the gray bits be the incremental syndrome, i.e. least significant bits, needed to correctly decode using the predictor

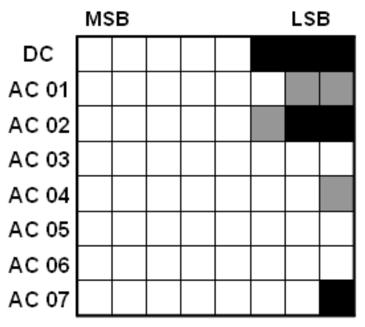

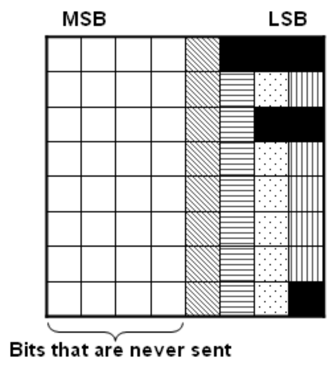

(a) (b)

Figure 3.6: Bit plane representation for DCT coefficients: (a) Bits marked black are the ones that cannot be inferred from the best predictor. Bits marked grey are the additional ones that cannot be inferred from the second best predictor. (b) Bits marked in the same pattern are LDPC encoded together.

from Frame $(t-2)$. Another way to interpret them is that these bits will be in error after we decode $\{\hat{X}_i^j(t)\}_{j=1}^{64}$ using only the baseline syndromes and $\{X_i^{j''}(t-2)\}_{j=1}^{64}$ as side information. But once we correct these bits, decoding will succeed.

The distributed source coding theory requires knowledge of the statistical correlation between the source and the side information, i.e. the statistics of $Z_i(t)$, at both the encoder and the decoder. In this context, this assumption implies that both the encoder and the decoder know the location of these gray bits. This is, however, not the case in practice due to the highly non-stationary nature of video data. In fact, only the encoder knows the location of the gray bits. Thus, we will treat the gray bits as bits in error and solve an error correction, instead of erasure, problem. We can use off-the-shelf state-of-the-art channel coding solutions, such as the LDPC codes. As partially shown in Figure 3.6(b), we chain each bit plane across different coefficients and all the blocks within the frame except for intra and skip blocks and apply an LDPC code with an appropriate rate. We exclude the bits that have already been transmitted in the baseline layer, i.e. the ones marked black in Figure 3.6(a) and (b) as prescribed by the illustrative example.

The LDPC rate is determined in the following way. For each bit plane, the encoder has perfect knowledge of how many bits will be in error if the second predictor is used as side information. Specifically, the bit error rate of each bit plane is the fraction of gray bits. Suppose for one bit plane, the fraction of gray bits is p_e. Using the finite block length analysis, we can target a certain decoding failure probability and numerically solve for a rebate factor h_b such that robustness decoding will succeed as long as h_b fraction of the blocks in Frame $t-1$ are correctly decoded. The LDPC rate for the bit plane should then be designed to target $p_e \cdot h_b$ bit error rate. Note that p_e is different for each bit plane, but h_b is the same for all bit planes in a frame. h_b varies from frame to frame within each GOP. Assuming the I-frame is always successfully transmitted, h_b can be computed offline once and stored in the encoder for a certain number of packets per frame. If $p_e \cdot h_b$ is sufficiently small, we skip the robustness layer encoding for that bit plane. We can transmit the bit error rate for each bit plane using negligible rate.

We store a bank of 9 LDPC codes with different compression rates. These degree distributions were obtained either from the LTHC [6] online database or generated (in [39]) using the EXIT charts [8] based design technique. For convenience, the source coding compression rates of the codes, to two significant digits, are as follows: 0.15, 0.20, 0.30, 0.40, 0.50, 0.63, 0.73, 0.82, 0.90. Please see [39] for detailed degree distributions.

In summary, the robustness layer contains both motion vectors for the second predictor and parity bits for a selected number of least significant bit planes generated by LDPC codes and their corresponding bit error rates.

3.3.2 Decoder

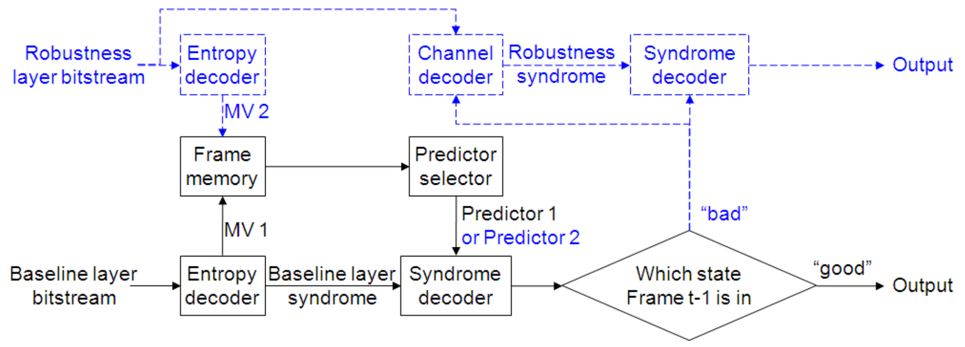

Figure 3.7: Block diagram for the decoder. Components in solid black lines belong to the baseline layer while components in dashed blue lines belong to the robustness layer.

Figure 3.7 depicts the block diagram for the decoder. Components in solid black lines belong to the baseline layer while components in dashed blue lines belong to the robustness layer.

Baseline layer

The baseline decoder is almost like an inverse of the baseline encoder and follows the following steps:

- **FEC decoding**: This will recover all the lost packets in a good frame state with high probability.
- **Entropy decoding**: Recovers motion vectors for the best predictors and base-

line syndromes for DCT coefficients.

- **Syndrome decoding**: Based on decoder's knowledge regarding past packet drop history, syndrome decode a block if its best predictor has been correctly decoded. Since a predictor block could overlap with up to four 8×8 non-overlapping encoding blocks, it will be considered correctly decoded only if all these overlapping encoding blocks have been correctly decoded. The decoder syndrome-decodes each coefficient to be the codeword closest to the side information in the indicated coset. This step also includes an estimation process at the end that is standard to Wyner-Ziv decoding to exact estimation gain. For each block whose best predictor is available, the decoder marks the block as correct. Otherwise, it marks the block as uncertain and leaves the decoding to the robustness layer.
- **Inverse quantization**.
- **Inverse DCT**.

Clearly, if there are no packet drops, baseline layer decoding suffices to reconstruct the entire video.

Robustness layer

If the current frame is in a bad state, the lost packets cannot be recovered in general. We carry out standard error concealment and mark these blocks as lost. We will not attempt robustness layer decoding either as prescribed by the illustrative example. If the frame is a good state, and there are past errors to clean up due to previous bad frame states, robustness layer decoding works as follows:

- **Entropy decoding**: Recover the motion vectors for the second predictor.
- **Syndrome decoding for uncertain blocks**: For each block whose best predictor is not available, if the second predictor has been correctly decoded, syndrome-decode this block using only the baseline syndrome with the second predictor being the side information. If neither of the predictors is correctly decoded, the best predictor, though corrupted, is used as side information to syndrome-decode the block using only the baseline syndrome.
- **Syndrome decoding to clean up past errors**: After syndrome-decoding the whole frame once, we use the partially erroneous reconstruction (in DCT domain) as the side information to the robustness layer decoder. Starting from the least significant bit plane, we carry out bit plane decoding using the LDPC parity bits in the robustness layer. After each LDPC decoding, each block that is mark uncertain is syndrome-decoded on a coefficient-basis again (using possibly newly corrected syndromes). The result is used as side information for the decoding of the next bit plane. If all LDPC decoding succeeds, which should happen with high probability, all the uncertain blocks are re-marked as correct.
- **Estimation**, **inverse quantization** and **inverse DCT** for blocks that changed status from uncertain to correct.

One significant advantage of such a layered approach is that starting with a new I-frame, the decoder does not need the robustness layer at all until it experiences a bad frame state. This greatly reduces overall decoding complexity as the base layer is entropy-coded and multi-level syndrome decoding has very low complexity.

3.4 Simulation results

3.4.1 Compression results of baseline layer

We first demonstrate that when there is no channel loss, the baseline layer of the proposed system suffices to reconstruct the original video and closely matches the compression efficiency of H.263+. The result is shown in Figure 3.8 for the first 15 frames of Foreman and Tempete sequences. Both sequences are of dimension 355×288, GOP size 15, and frame rate 30 frames per second.

The compression efficiency of the baseline layer is important as for download applications, users can simply download the baseline layer of the video without the robustness layer at all. The baseline layer decoding complexity is also low as mentioned earlier.

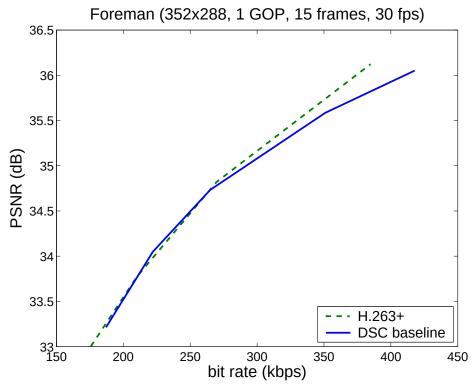

(a)

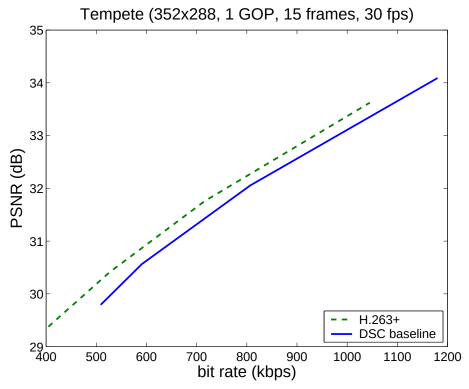

(b)

Figure 3.8: Compression efficiency comparison between the baseline layer of the proposed system and H.263+ for: (a) Foreman sequence (352×288, 1 GOP of 15 frames at 30 fps), and (b) Tempete sequence (352×288, 1 GOP of 15 frames at 30 fps).

3.4.2 Robustness results of robustness layer

We now demonstrate the effect of the robustness layer for low-latency transmission over channels with bursty errors. Three systems are compared:

1. Proposed system with its baseline layer encoded at rate R and the robustness layer at rate ΔR,
2. H.263+ encoded at rate R' such that the decoded video quality is the same as that of System (1) when there are no packet drops and $R + \Delta R - R'$ allocated to FEC (we use Reed-Solomon codes),
3. H.263+ encoded at rate $R + \Delta R$ with random intra refresh enabled such that the decoded video quality is the same as that of System (1) when there are no packet drops.

The latency constraint is 1 frame, as in, the decoder must immediately display the received frame.

Two-state channel

First, we simulate the same two-state channel model as described in Section 3.2. In the "good" state, we simulate 3% independent packet drops. In the "bad" state, we simulate 30% independent packet drops. We used high-motion sequences as they are the most prone to the effect of drift and present the biggest challenges in robust video transmission. We use the Stefan sequence (352×240, GOP = 15, 15 fps) with $R = 1.1$mbps and $\Delta R = 360$kbps and Football sequence (352×240, GOP = 30, 15 fps) with $R = 900$kbps and $\Delta R = 300$kbps.

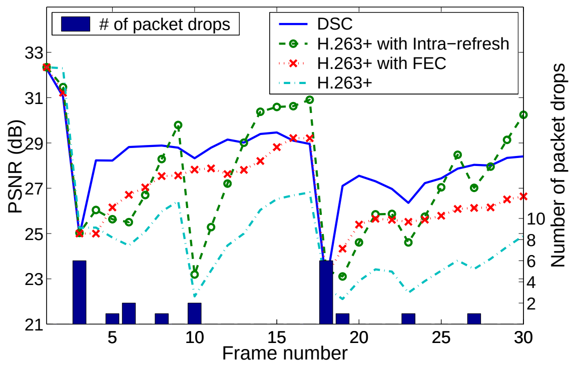

(a)

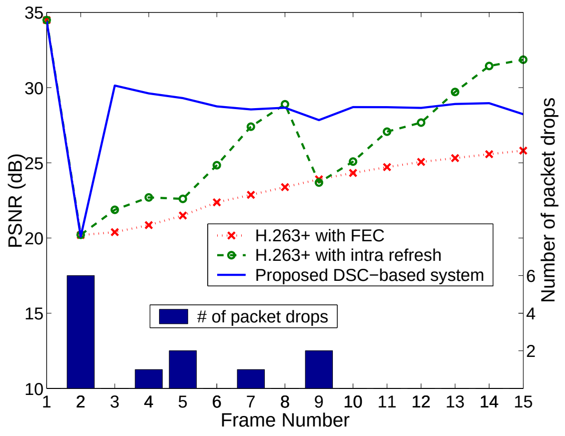

(b)

Figure 3.9: Robustness performance of the different schemes for (a) Football (352×240, 1 GOP of 15 frames at 30 fps) and (b) Stefan (352×240, 1 GOP of 15 frames at 30 fps) sequences using the two-state channel. In a good state, we simulate 3% independent packet drops. In a bad state, we simulate 30% independent packet drops. The bar diagram represents the number of actual packet drops in each frame. For Stefan, $R = 1.1$mbps (15 fps), $\Delta R = 360$kbps. For Football, $R = 1.0$mbps (15 fps), $\Delta R = 330$ kbps. In (a), we also added the performance of H.263+ baseline encoded at a higher rate.

Figure 3.9 show both the PSNR and the number of packet drops for each frame. As we can see, the proposed system experiences a dip in PSNR after each burst of packet drops. This is because the proposed system does not attempt to clean up errors in a bad channel state. However, the quality recovers drastically immediately, i.e. there is a 3 - 10 dB quality recovery in the frame right after a burst of packet drops, depending on how severely the frame is corrupted in the bad state. Since we do not send robustness syndrome for the SKIP blocks, there will be some residual errors. But the effect is not obvious as evidenced by the high recovered PSNR.

For the H.263+ with FEC system, on the other hand, we see that when a burst of packet drop exceeds the correction capacity of FEC codes, such as in Frame 2 in Figure 3.9(a) and Frame 3 and 18 in Figure 3.9(b), the performance degradation is significant. After the severe quality drop, the error effect slowly reduces but propagates through the rest of the group of picture, causing drift. While intra refresh, i.e. System (3), can also quickly recover PSNR after a burst of packet drop, it still takes a long time for the entire frame to be refreshed. In the mean time, the refreshed blocks look perfect while the rest of the frame suffers poor decoded quality. Thus even though the PSNR increases steadily after packet drops, there are oftentimes persistent erroneous areas.

Figure 3.10 shows Frame 3 and 4 of the Football seuqnce using the different systems. We can see that the proposed system has the most instant drift reduction in Frame 4 after experiencing a bust of packet drops in Frame 3.

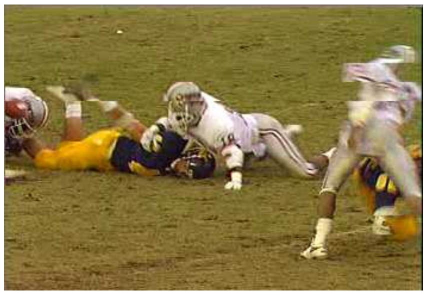
(a) Frame 3: H.263+ with FEC

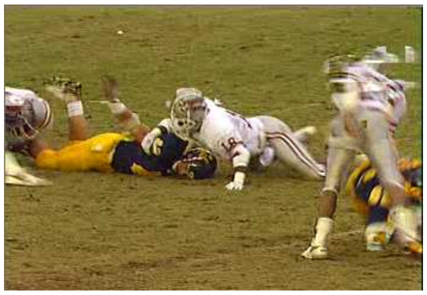
(b) Frame 4: H.263+ with FEC

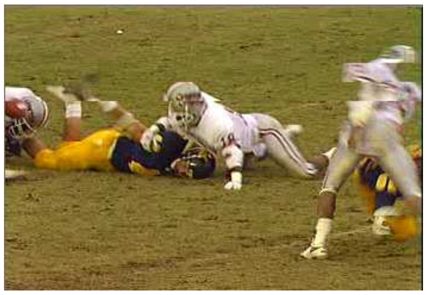
(c) Frame 3: H.263+ with intra refresh

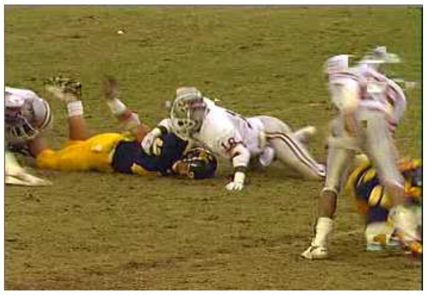
(d) Frame 4: H.263+ with intra refresh

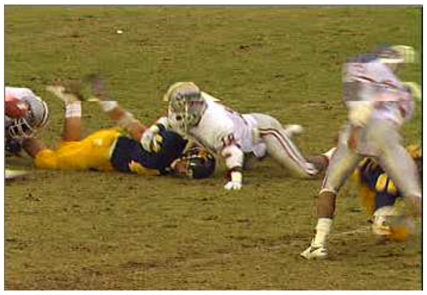
(e) Frame 3: proposed system

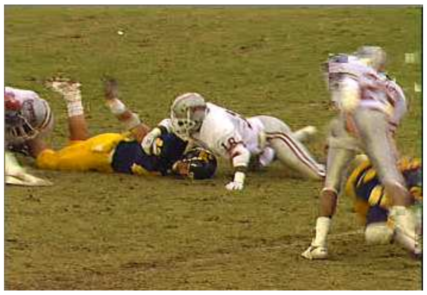
(f) Frame 4: proposed system

Figure 3.10: Frame 3 and 4 of Football sequence using three different systems. The proposed system has the most instant recovery from packet drops in Frame 3.

Simulated CDMA2000-1x channel

We then validate the accuracy of our channel model and the effectiveness of the proposed scheme by using a simulated wireless channel conforming to the CDMA 20001x standard. Figure 3.11 shows very similar behavior to that of the simulated two-state channel. Again, the proposed system is able to achieve an instantaneous quality recovery right after a burst of packet drops.

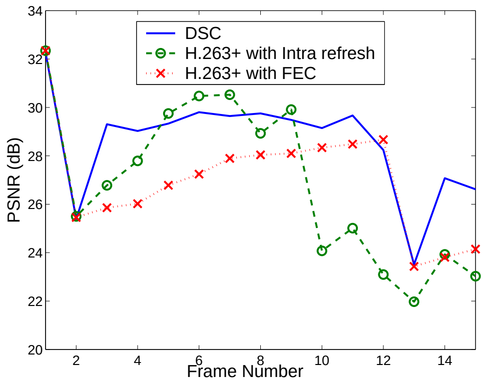

(a) Football

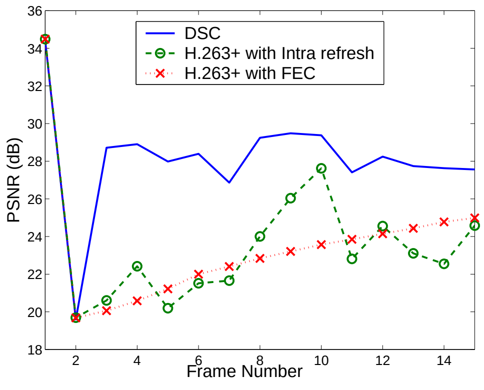

(b) Stefan

Figure 3.11: Robustness performance of the different schemes for Football (352×240, 1 GOP of 15 frames at 30 fps) and Stefan (352×240, 1 GOP of 15 frames at 30 fps) sequences using a simulated wireless channel conforming to the CDMA 2000 1x standard. Again, for Stefan, $R = 1.1$mbps (15 fps), $\Delta R = 360$kbps. For Football, $R = 1.0$mbps (15 fps), $\Delta R = 330$ kbps. In (a), Football sequence was used and the average packet drop rate is 7.4%. In (b), Stefan sequence was used and the average packet drop rate is 7.1%.

Chapter 4

Conclusion and future work

In this part of the thesis, we have focused on the problem of low-latency video streaming over lossy packet networks. We have presented a distributed source coding based video coding system that enables robust low-latency video transmission over channels characterized by bursty packet drops, such as wireless networks. Based on a generalization of the classical Wyner-Ziv setup, the proposed distributed video codec is characterized by an inherent system uncertainty about the "state" of the relevant side information available at the decoder. The compressed bitstream comprises of a baseline layer that suffices to reconstruct the video when there are no packet drops and a robustness layer that is used to combat transmission errors. By taking a joint source-channel coding approach, the proposed system can tune to both the source content as well as to the network loss characteristics.

The key ideas of the proposed system are the following:

- We choose to give up perfectly reconstructing frames that are transmitted under poor channel conditions. Instead, we aim to recover decoded video quality immediately after a burst of packet drops.

- We associate each block with more than one predictors and aim to decode successfully as long as one of these predictors are correctly reconstructed at the decoder. The strong temporal correlation of video data provides the perfect diversity in time to make this scheme efficient.
- Instead of coding according to the worst predictor that the current block is associated with, we take advantage of the fact that the best predictor will be available at the decoder most of the time and achieve better compression efficiency.
- The decoder can make intelligent choice regarding which predictor to use based on its knowledge of previous blocks' decoding status.

While some of these philosophies can be used in the conventional predictive coding framework as well, the distributed source coding framework allows the most efficient implementation of these ideas in terms of compression efficiency for lossy coding. In this thesis, we have presented a theoretical analysis of the proposed system under a simplified analytically tractable model and quantified the gains with respect to predictive codecs when the transmission channel is characterized by bursty packet drops. We implemented the proposed system and verified its effectiveness of the proposed system through simulations using both synthetic and real-world channel simulators.

The work in this part of the thesis suggests several avenues of further study. We itemize some of these directions here.

- The robustness advantages of the proposed system need to be studied for more accurate video models.

- By using rate-adaptive LDPC codes for the robustness layer, one may break the robustness layer into several layers to target different packet drop statistics. This may be useful in a layered multicast setup, like in [30].

- For a video coder, there is typically a complexity-performance tradeoff. In the context of the proposed system, coarser motion search will naturally lead to lower compression efficiency. However, in a DSC framework, this means that predictors of worse quality will also lead to correct reconstruction of the current block. It is worthwhile to study how to exploit and quantify this increased robustness with lower encoder complexity.

- Correlation estimation under arbitrary channel conditions remains an open question in general.

We hope this work will spur further research in the area of robust video transmission using distributed source coding principles. We believe the DSC framework has the potential of leading to video codecs that are fundamentally more suitable for the new generation of video applications.

Part II

Video distribution over collaborative peer-to-peer networks

Chapter 5

Introduction

Internet video is poised to be *the next big thing.* It is predicted that the revenue from Internet video will grow with an annual growth rate of 49.7% from $0.63 billion in 2006 to $4.74 billion by 2011 [22]. As consumers spend more and more time watching videos online, they are no longer content with being restrained to their computers. Consequently, the demand to get Internet video into the living room is at a record-high. This demand fuels the increasing popularity of services (Amazon Unbox, Netflix On Demand, etc.), as well as devices with such capabilities (Microsoft Media Center, Apple TV, TiVo, etc.). Once in the living room, consumers quickly realize that they prefer to go beyond YouTube's limited quality and enjoy SD or even HD video.

However, providing high-quality Internet video with a traditional client-server model is very costly [31]. The ever mounting demand is adding significant pressure to existing server-based infrastructures, such as data centers and content distribution networks (CDNs), which are already heavily burdened. As a result, highprofile failures, such as MSNBC's democratic presidential debate webcast mess [17] and the Operah web show crash [26], are not uncommon. The Internet itself is even predicted to melt down if online video does become mainstream [5].

Fortunately, on the heels of such crisis comes the help of peer-to-peer (P2P) technology. A P2P network enables a community of users (nodes) to pool their resources (such as content, storage, network bandwidth, disk capacity, and CPU power) in a *self-organizing* and *decentralized* fashion, thereby providing access to larger archival stores, faster data acquisition, more complex computations, etc. More importantly, as nodes arrive and demand on the system increases, the total capacity of the system also increases. This allows a P2P system to scale gracefully to the number of nodes, unlike the client-server framework in which a fixed number of servers serve all the peers (Figure 5.1).

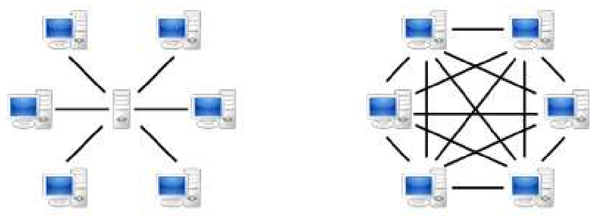

(a) Client-server framework (b) P2P network

Figure 5.1: A server-based network vs. a peer-to-peer network.

There are many aspects to improving a peer-to-peer network. In Chapter 6 of the dissertation, we study how to improve the performance of P2P video download through a higher level of collaboration among peers. Specifically, we study efficient resource utilization of *helper* nodes. These are nodes that are not interested in the file being shared but have spare bandwidth resources and are willing to share. We propose a light-weight, distributed protocol that is backwards-compatible with the popular BitTorrent file sharing protocol and analyze the steady-state system performance using a fluid model as in Qiu and Srikant [38]. We then extend the framework to design an algorithm for efficient utilization of helpers for P2P live video multicast.

Throughout this part of dissertation, the terms "node", "peer", and "user" are used interchangeably, according to the context, to refer to the entities that are connected in a P2P network.

5.1 Peer-to-peer networking overview

Definition The definition for "peer-to-peer" can vary depending on the broadness that is attached to the term. The strictest definitions of "pure" peer-to-peer refer to totally distributed systems, in which all nodes are completely equivalent in terms of functionality and tasks they perform. In the context of this dissertation, we adopt a broader and widely accepted definition in [42], "peer-to-peer is a class of applications that take advantage of resources – storage, cycles, content, human presence – available at the edges of the internet."

Classification by application Peer-to-peer architectures have been employed for various application categories, which include, but are not limited to, the following.

- Collaboration and Communication. This category includes systems that provide the infrastructure for facilitating direct, usually real-time, communication and collaboration between peer computers. One of the most well-known examples is the Internet telephone company Skype [4].

- Distributed Computation. This category includes systems whose aim is to take advantage of the available peer processing power, i.e. CPU cycles. This is achieved by breaking down a computational intensive task into small work units and distributing them to different peer computers. Peer computers execute their corresponding work unit and return the results. Central coordination is required for breaking up and distributing the tasks, as well as collecting the results. Examples of such systems include Berkeley's SETI@home project [3] and distributed.net, which is a world-wide distributed computing effort that is attempting to solve large scale problems using otherwise idle CPU time.

- Content Distribution. Most of the current P2P systems fall within the category of content distribution, which includes systems and infrastructures designed for the sharing of digital media and other data between users. Peer-to-peer content distribution systems range from relatively simple direct file-sharing applications to more sophisticated systems that create a distributed storage medium for publishing, organizing, indexing, searching, updating, and retrieving data. There are numerous such systems and infrastructures, including Gnutella [1], KaZaA [2], and BitTorrent [14].

In this section, we review content distribution over P2P networks. The operation of any P2P content distribution system relies on a network of peer computers and connections among them. This network is formed on top of – and independently from – the underlying physical computer network, and is thus referred to as an "overlay" network. Overlay networks can be distinguished in terms of their centralization and structure.

Classification by degree of overlay centralization There are three types of P2P architectures based on the degree of centralization of the overlay network: purely decentralized architecture, partially centralized architecture, and hybrid decentralized architecture. In a *purely decentralized architecture*, all nodes in the network perform exactly the same tasks, acting both as servers and clients, and there is no central coordination of their activities. The basis of a *partially centralized architecture* is the same as with purely decentralized systems. Some of the nodes, however, assume a more important role, such as acting as local central indices for files shared by local peers. These so-called "supernodes" are assigned various roles by the network depending on the application. These supernodes do not constitute single points of failure for a P2P network, since they are dynamically assigned and, if they fail, the network will automatically take action to replace them with others. Finally, in a *hybrid decentralized architecture*, there is a central server facilitating the interaction among peers by maintaining directories of participating peers, content metadata, and sometimes the content source itself. Although the end-to-end interaction and file exchanges may take place directly between two peer nodes, the central servers facilitate this interaction by performing the lookups and identifying the nodes that are sharing the relevant content.

Classification by overlay structure *Unstructured* overlays build a random graph and use flooding or random walks on that graph to discover data stored by overlay nodes. *Structured* overlays assign keys to data items and build a graph that maps each key to the node that stores the corresponding data. While structured overlays can provide guarantees on quality of service, e.g. the maximum number of hops to locate the desired content, unstructured overlays are widely used in popular applications, such as Gnutella and BitTorrent. This is because unstructured overlays are easy to maintain, resistent to peer churning, and can perform arbitrarily complex queries.

In this dissertation we study two important forms of Internet video distribution: download (e.g. downloads at iTunes store) and live multicast (e.g. NBC's web broadcast of the 2008 Olympic games). Each distribution method has its own unique characteristics.

For download, peers aim to obtain a certain file that is pre-generated. Peers may start the download any time they want, quit any time they want, and may finish downloading at different times. From an end user's point of view, the main performance metric is the amount of time it takes to download the entire file.

For multicast, peers may join the system at different times but they watch the same content at the same time. In other words, peers have synchronous or at least loosely *synchronous* playback points. The content can be either pre-generated or being generated in real-time. Nonetheless, unlike download, there is not a finishing point for live multicast. Peers can stay in the system for as long as they want and the content they are viewing is constantly updated.

The biggest difference between P2P download and streaming applications is that for streaming applications, each packet has a specific delivery deadline. This difference dictates that streaming applications need to have more efficient resource allocation and topology building schemes. We will examine these topics in more detail in Section 6.3.3.

Chapter 6

Helper-assisted peer-to-peer video distribution

In this chapter, we study how to improve the performance of P2P video download through a higher-level collaboration among peers. Specifically, we study efficient resource utilization of helpers, which are nodes that are not interested in the file being shared but are willing to share their spare bandwidth resources. We propose a light-weight, distributed protocol that is backwards-compatible with the popular BitTorrent file sharing protocol. We demonstrate the efficiency of the proposed protocol both analytically and empirically. We also analyze the steady-state system performance using a fluid model of Qiu and Srikant [38] and verify the validity of the fluid-model analysis through simulations.

We first review the BitTorrent protocol, which is an important building stone of the proposed helper protocol.

6.1 The BitTorrent protocol

BitTorrent [14] is a massively popular peer-to-peer (P2P) file sharing protocol and makes up a large fraction of Internet traffic [34]. By the definition of P2P, its goal is to enable efficient distribution of large files by utilizing the upload bandwidth of the downloading peers. In a nutshell, a file of interest is broken into equal-sized pieces (or chunks). Peers that are interested in the file form a peer-to-peer overlay network (called a *swarm*). Each peer downloads and uploads these pieces to multiple peers simultaneously.

There are two types of peers in a BitTorrent file sharing swarm: *seeders* and *leechers*. Seeders are peers that have the entire file but stay in the system to upload to others. Leechers are peers that have not finished downloading the entire file. Another important component of a BitTorrent file sharing swarm is a *tracker*. A tracker is a server that coordinates the file distribution. It keeps track of all the peers in the swarm.[1]

The content provider breaks the file into a number of equal-sized pieces, typically between 64 KB and 4 MB each. It creates a checksum for each piece and records it in a meta data file (with the `.torrent` suffix), called a torrent file. This torrent file also contains the URL of the tracker, and other information regarding the file, including its name, overall size, and the size of each piece. The content provider then publishes the torrent file on a Web site and starts a BitTorrent client with a full copy of the file of interest as the original seeder.

A new peer interested in a particular file browses the Web to find a matching

[1]Recent BitTorrent softwares also support trackerless systems where peers act as distributed trackers using distributed hash table techniques.

torrent. It connects to the indicated tracker to obtain a subset of existing peers. It tries to establish connection with a certain number of them, which become its neighbors. Peers contacts the tracker whenever the number of its neighbors falls below a certain threshold.

Local rarest first piece selection: Each peer maintains an availability map of all the pieces of the file and reports it to all of its neighbors. Peers request pieces they do not have from their neighbors using these availability maps. It is important to select pieces to download in an efficient order to maximize utilization of peers' upload bandwidth. The most popular basic strategy is called 'local rarest first', where peers choose to download the rarest piece in its one-hop neighborhood first.

Tit-for-tat resource allocation: Peers allocate their resources, i.e. upload bandwidth, by following a variant of tit-for-tat strategy. Specifically, a peer uploads to, or *unchokes* in BitTorrent terminology, a fixed number (say m) of neighbors that are uploading to itself the fastest.

Optimistic unchoking for topology optimizing: To discover better connections than the currently active ones, peers periodically chooses a random neighbor to upload to. This process is called optimistic unchoking. If, in return, this new neighbor starts uploading to the peer faster than some of the existing active connections, the peer will stop uploading, or *choke* in BitTorrent terminology, to the neighbor it is now downloading from at the lowest rate, thereby maintaining a constant number of active connections.

Upon finishing downloading a file, a leecher becomes a seeder and may choose to stay in the swarm to serve other peers or to leave.

6.2 Helper-assisted peer-to-peer video download

For a BitTorrent-like file sharing system, the system throughput is capped by the minimum of the total system upload bandwidth and the total system download bandwidth [38]. However, a large population of Internet users today have asymmetric Internet service, such as ADSL and cable, and have much lower upload than download bandwidth. This makes peers' total available upload capacity oftentimes the most prominent constraint of a peer-to-peer network. We propose to overcome this practical constraint by promoting a higher-level collaboration among network peers to optimize performance of a uplink-scarce collaborative networks beyond that can be achieved by a conventional P2P network. One important observation is that at any given time, while there are peers exhausting their upload bandwidth sharing data, there are also numerous peers with spare upload capacity who may be idling. This is a direct result of the statistical multiplexing property of a large-scale system in the sense that peers have not only different physical capabilities but also different behavioral characteristics. We call such peers helpers. Helpers represent a rich untapped resource, whose upload bandwidth can be exploited for increasing the total system upload bandwidth and hence easing the performance bottleneck.

Before introducing the proposed helper protocol, we first review some related work that share similar philosophy as ours.

6.2.1 Related work

Guo et. al. [24] briefly explored the idea of inter-torrent collaboration, and described a scheme where peers may download pieces of a file in which they are not interested in exchange for pieces of a file they want to download. For example, let let Peer A be a leecher of File 1. Peer B, C, and D are leechers of File 2. B, C, and D also has parts of File 1 but are not interested in downloading File 1 at the moment. Peer A would like to download pieces of File 1 from B, C, and D but has nothing in exchange. Peer A thus downloads a few pieces of File 2 and upload them to B, C, and D in exchange for pieces of File 1. This is essentially an incentive for seeders of a particular file remain a seeder for that file for a longer period of time. However, across different swarms, this scheme does not increase the overall system throughput like the proposed helper scheme. Therefore, if both File 1 and File 2 have reasonably sized file sharing swarms, there will not be any performance gain. However, it is useful if the seeders of a particular file become too scarce.

The idea of helpers was first introduced by Wong [49]. Their definition for helpers is in fact exactly the same as ours – helpers are peers that are not interested in the content being distributed but are willing to contribute their spare upload bandwidth. They introduce a heuristics based helper protocol that is quite different from ours and verify the effectiveness of the scheme through simulations. Clearly, a helper needs to download before they can upload. In [49], a helper aim to upload each piece it downloads at least u times, where u is a heuristically predetermined number called *upload factor*. This way, helpers can guarantee to upload more than they download and contribute to the system. To make sure each piece it downloads is uploaded at least u times, a helper keeps track of the number of times each piece has been upload and considers a piece *unfulfilled* if the piece has not been uploaded u times. The helper downloads a new piece when the number of unfulfilled piece is below a certain predetermined limit. As we show in our analysis and simulation, this strategy is wasteful because the longer a peer stays in the system, the more pieces it will download, which is unnecessary for helpers to keep their upload bandwidth fully utilized.

In the “Tribler” [35] system, Pouwelse et al. proposed a novel paradigm for P2P file sharing networks based on social phenomena such as friendship and trust. In their 2Fast file sharing protocol, a peer trying to download a file actively recruits its “friends”, such as other peers in the same social network, to help *exclusively* with its download. Specifically, a peer will assign a list of pieces to obtain for each of its helpers. These are the pieces that it has not started downloading. The helpers will try to obtain these pieces just like regular leechers and upload these pieces to the peer they are helping. In such a scheme, peers with more friends can indeed benefit greatly and enjoy a much reduced file download time. However, the constraint that helpers only aim to help a single peer requires the helpers to download much more than necessary to remain helpful to this peer. We remove this constraint and thus provide much more efficient use of helpers resource as will be become more apparent after we introduce the proposed helper protocol. However, we feel the social network based incentivising scheme works nicely with the philosophy of the proposed scheme. Instead of looking at it from a leecher’s point of view and having each leecher recruit many helpers that share similar interests to help itself exclusively, we can look at it from the helpers’ point of view. Essentially, as a helper, it may be willing to facilitate the distribution of files that its social circle is interested in. For example, peers that are interested in the Disney channel may choose to help the distribution of the latest episode of High School Musical even though they do not want it themselves and they do not have a particular friend they want to help.

6.2.2 BitTorrent-compatible helper protocol and its efficiency

We now describe the proposed helper protocol that is backwards-compatible with the BitTorrent protocol. We continue to use some of the terminologies from BitTorrent. Namely, a leecher is a peer who has not finished downloading the entire file. A seeder is a peer who has obtained the entire file and is staying in the system to upload to the leechers.

A helper joins a swarm just like a regular leecher. The download mechanism of a helper is the same as that of a regular peer except

- a helper only downloads k pieces of the file, with k being a fixed small number that does not scale with the number of pieces the file is broken into;
- helpers are not allowed to download from each other.

We will explain in detail the reason behind these design choices shortly.

In choosing which k pieces to download, different strategies can be adopted. We found both random and local-rarest-first [14] mechanisms to be equally effective. Once a helper finishes downloading k pieces of the file, it stops downloading. We call such a helper a *microseeder*. At this time, it reports to the tracker and obtains a list of regular peers. Helpers (including microseeders) implement the same choking/unchoking algorithm that is adopted by any BitTorrent client. However, once a microseeder sees that a neighbor has already obtained all the k pieces it has to offer, it will automatically disconnect from the neighbor.

We note that in this protocol, we require that helpers be aware of each other. As mentioned earlier, there is no need for existing BitTorrent peers to be modified.

We now show analytically that microseeders' upload bandwidth can be almost fully utilized even if it only has a small fixed number of pieces k of a file. Let the file be broken into N equal-sized pieces.

Proposition 1. *Assuming the number of pieces a random leecher has is uniformly distributed in* $\{0, 1, \ldots, N-1\}$ *and* $k \ll N$*, the average probability that a microseeder has at least one piece that a leecher does not have is* $\frac{k}{k+1}$.

Proof.

$$\begin{aligned} & \mathbb{P}\left(\text{Leecher } i \text{ needs at least 1 piece from Microseeder } j\right) \\ = \;& 1 - \mathbb{P}\left(\text{Leecher } i \text{ needs no piece from Microseeder } j\right) \end{aligned}$$

Let n_i denote the number of pieces a random leecher i has acquired. Since n_i is uniformly distributed in $\{0, 1, \ldots, N-1\}$, we have

$$\begin{aligned} & \mathbb{P}\left(\text{Leecher } i \text{ needs no piece from Microseed } j\right) \\ = \;& \mathbb{P}\left(\text{Leecher } i \text{ has all pieces of Microseed } j\right) \\ = \;& \sum_{n_i=k}^{N-1} \frac{1}{N} \mathbb{P}\left(\text{Leecher } i \text{ has all pieces of Helper } j | n_i\right) \\ = \;& \sum_{n_i=k}^{N-1} \frac{1}{N} \cdot \frac{\binom{N-k}{n_i-k}}{\binom{N}{n_i}} \\ = \;& \frac{N-k}{N(k+1)} \\ \rightarrow \;& \frac{1}{k+1} \text{ if } N \gg k \end{aligned}$$

□

If a helper has m neighboring peers, the probability that at least one of its neighbors needs at least a piece from the helper is $1 - (\frac{1}{k+1})^m$. Since this value is close to 1 with a reasonably small m, the upload capacity of the helper is almost always utilized even if it only downloads a very small number of pieces. Note that this probability is also unrelated to N as long as $k \ll N$. This means the number of pieces a helper has to download (k) in order to maintain high uplink utilization needs not scale with the size of the file.

In practice, in order to reduce the amount of connection and query overhead, we would like to ensure that every leecher that a helper connects to will need at least one piece from the helper with high probability (say p). Intuitively, for any helper, the probability of finding such a peer is high if it looks among peers who have finished only a small portion of the download. If the tracker keeps track of the rough download progress of all the peers in the swarm by periodically collecting data from the peers,[2] then when a helper queries the tracker for a list of peers, the tracker could reply with a list of leechers who have finished downloading no more than a limited number of pieces (say l). Given a target probability p and the number of pieces k a microseeder has, we can solve for l from

$$1 - \frac{\binom{N-k}{l-k}}{\binom{N}{l}} \geq p.$$

There is not much incentive for a leecher to take advantage of the system by misreporting its download progress. Because the probability of being helped by a microseeder becomes much lower once a leecher has downloaded a large fraction of the file.

As mentioned earlier, we disallow helpers to download from each other. This

[2]In fact, the BitTorrent protocol does allow the tracker to keep track of the download progress of the peers [14].

is because we would like the helpers to have a diverse collection of pieces. Intuitively, if all the helpers have the same pieces, their helpfulness would be much reduced. The reason is that if helpers have the same pieces, then very quickly all the leechers in the system will have acquired these pieces, rendering helpers useless. Our simulations show that this restriction has negligible impact on the rate at which helpers turn into microseeders.

6.2.3 System performance analysis using fluid model

We now analyze the steady-state system performance with and without helpers. We model the steady-state behavior of the system with homogeneous peers using the "fluid model" proposed in [38] and make some important corrections.

We first consider Following the model in [38], we have the following assumptions:

- The peer arrival process is Poisson with a fixed rate.
- The peers are homogeneous and have the same upload bandwidth and the same download bandwidth.
- The peers download at the same rate when they are downloading. This rate is the total upload bandwidth from all the participating peers divided up equally among the downloading peers. Thus we assume that the instantaneous download rate is the same for all the downloading users.
- We treat the number of peers and seeders in the system as non-negative real numbers.

- A peer may abort its download. Once it aborts the download, it will never return.
- Once a seeder leaves the system, it will never return.[3]

We present the analysis for the case where peers' upload bandwidth is smaller than their download bandwidth. This is the case in reality and also the scenario of interest. We define the following quantities as in [38]:

- μ Upload bandwidth of the peers (b/s)[4]
- λ Arrival rate of peers (users/s)
- $x(t)$ Number of peers downloading at time t
- $y(t)$ Number of seeders in the system at time t
- θ Patience factor of peers (1/s). If a peer does not finish downloading the entire file after some time, it aborts the download. The amount of time is modeled to be independent across peers and exponentially distributed with mean $1/\theta$.
- γ Patience factor of seeders (1/s). Having finished the download, each seeder remains in the system for a while longer. The amount of time they stay is an exponential random variable with mean $1/\gamma$, also independent across peers.
- η Efficiency factor of peers who are downloading. This is the average probability that a downloading peer has at least one piece that one of the peers it is connected to does not have.

[3]This assumption can be easily relaxed.
[4]All bandwidths are normalized so that the size of the file can be taken to be unity.

In addition, we define $w(t)$ (b/s) as the bandwidth "wasted" by peers who abort before downloading the whole file. This wastage was not accounted for in the model in [38]. By leaving out this term, the bandwidth consumed by the aborting peers was also counted towards contributing to seeder creation. This will lead to inflated performance. The discrepancy can be significant in cases where a significant number of peers abort without downloading the whole file.

We first describe the rate at which the number of leechers in the system changes. This is equal to the rate at which leechers enter the system minus the rate at which leechers disappear. The rate at which leechers disappear is equal to the leecher aborting rate plus the rate at which leechers turn into seeders. For a system without helpers, the total upload rate available is given by $\mu(\eta x(t) + y(t))$. Since the file size is normalized to unity and upload bandwidth is evenly divided among all leechers, $\mu(\eta x(t) + y(t)) - w(t)$ is the rate at which peers finish their downloads and turn into seeders. Hence we have:

$$\frac{dx(t)}{dt} = \lambda - \theta x(t) - [(\mu(\eta x(t) + y(t))) - w(t)] \tag{6.1}$$

Similarly, the rate at which the number of seeders in the system changes is equal to the rate at which seeders are generated minus the rate at which seeders leave the system. The rate at which seeders are generated is the same as the rate at which leechers become seeders. Thus,

$$\frac{dy(t)}{dt} = [(\mu(\eta x(t) + y(t))) - w(t)] - \gamma y(t) \tag{6.2}$$

In steady state, x(t), y(t) and w(t) are all constant. Let x, y, and w denote the steady-state values of $x(t)$, $y(t)$ and $w(t)$ respectively. The steady-state leecher download rate is then the total upload bandwidth divided by the number of leechers in the system, i.e. $\frac{\mu(\eta x+y)}{x}$. Consequently, the time taken by a peer to download the entire file in steady-state is given by

$$T_{\mathrm{dl}} = \frac{1}{\text{steady-state peer download rate}} = \frac{1}{\mu(\eta x + y)/x}. \tag{6.3}$$

If a leecher stays in the system for a shorter amount of time than T_{dl}, it will not have finished downloading the file and all the content it has downloaded will be wasted. θx is the average number of peers aborting per unit of time. Let $p_\theta(t) = \frac{1}{\theta}\exp(-\theta t)$, $t \geq 0$ be the exponential PDF of peers' staying time with mean $1/\theta$. $\frac{p_\theta(t)}{\int_0^{T_{\mathrm{dl}}} p_\theta(v)dv}$ is then the PDF of a peer's staying time t conditioned on the fact that the peer leaves the system before finishing downloading the whole file. $t \cdot \frac{\mu(\eta x+y)}{x}$ is the amount of bandwidth a peer has received when it aborts the download at Time t. The amount of wasted bandwidth per unit of time under steady-state can then be computed as

$$w = \theta x \int_0^{T_{\mathrm{dl}}} \frac{p_\theta(t)}{\int_0^{T_{\mathrm{dl}}} p_\theta(v)dv} \cdot t \cdot \frac{\mu(\eta x + y)}{x} dt = \theta\mu(\eta x + y)\frac{\int_0^{T_{\mathrm{dl}}} p_\theta(t)tdt}{\int_0^{T_{\mathrm{dl}}} p_\theta(t)dt}. \tag{6.4}$$

To obtain the steady-state solution, we set the steady-state conditions $\frac{dx(t)}{dt} = \frac{dy(t)}{dt} = 0$ and solve for x and y using (6.1), (6.2), (6.3) and (6.4). With the values of x and y in steady state, we can then obtain the steady-state average download time T_{dl} using (6.3). Note that the these equations can be solved only numerically due to the non-linearity of (6.4).

When the wastage term w is small enough to be ignored, we can analytically solve the equations above. The resulting file download time T_{dl} is given by

$$T_{\mathrm{dl}} = \frac{\gamma/\mu - 1}{\gamma\eta}. \tag{6.5}$$

As pointed out earlier, [38] ignores the effect of w. Furthermore, the expression of T_{dl} in [38] was in error, and hence differs from (6.5). In fact, the expression given in [38] is the leecher downloading time averaged over the peers who finish the download *as well as* the peers who abort without finishing their download. It is not the same as time taken to download the file averaged over only the peers who download the entire file, which is the value of interest. The computation in [38] results in an overly optimistic value for the download time. The error is the result of an inappropriate use of Little's Law. However, the conclusion in [38] that T_{dl} is independent of the peer arrival rate λ remains true whenever the effect of wastage is negligible.

We now analyze the system with helpers. We introduce the following additional notations:

- μ_h Upload bandwidth of the helpers (b/s)
- λ_h Arrival rate of helpers (users/s)
- $x_h(t)$ Number of helpers downloading at time t
- $y_h(t)$ Number of microseeds in the system at time t
- $w_h(t)$ Bandwidth "wasted" by helpers who abort before downloading k pieces (b/s)
- ε The proportion of the total upload bandwidth that is consumed by leechers. In our system, $\varepsilon = x(t)/(x(t) + x_h(t))$.
- θ_h Patience factor of helpers (1/s). The amount of time helpers stay in the system is independent across helpers and exponentially distributed with mean $1/\theta_h$. We use the same patience factor for both helpers who have not finished downloading k and microseeders. This is because helpers' objective is not

downloading. Thus, the number of pieces a helper has downloaded does not affect its decision whether to continue to stay in the system

- η_h Efficiency factor of helpers who have finished downloading their portion (defined similar to η)
- ρ The fraction of the file a helper download (k/N).

We make the simplifying assumption that helpers who have not finished downloading cannot contribute their upload bandwidth because (1) there are very few helpers that are not microseeders, and (2) when a helper first starts downloading, its upload bandwidth utilization efficiency is very low. It is later verified through simulation that this assumption has negligible impact. As a result, compared to a system without helpers, the additional amount of upload bandwidth contributed by the helpers is $\mu_h \eta_h y_h(t)$. The rate at which leechers become seeders is then

$$\varepsilon \left[\mu(\eta x(t) + y(t)) + \mu_h \eta_h y_h(t)\right] - w(t).$$

Similarly, the rate at which microseeders are generated is

$$\frac{(1-\varepsilon)\left[\mu(\eta x(t) + y(t)) + \mu_h \eta_h y_h(t)\right] - w_h(t)}{\rho}.$$

The fluid model can be updated as

$$\frac{dx(t)}{dt} = \lambda - \theta x(t) - [\varepsilon(\mu(\eta x(t) + y(t)) + \mu_h \eta_h y_h(t)) - w(t)] \tag{6.6}$$

$$\frac{dy(t)}{dt} = [\varepsilon(\mu(\eta x(t) + y(t)) + \mu_h \eta_h y_h(t)) - w(t)] - \gamma y(t) \tag{6.7}$$

$$\frac{dx_h(t)}{dt} = \lambda_h - \theta_h x(t) - \frac{(1-\varepsilon)[\mu(\eta x(t) + y(t)) + \mu_h \eta_h y_h(t)] - w_h(t)}{\rho} \tag{6.8}$$

$$\frac{dy_h(t)}{dt} = \frac{(1-\varepsilon)[\mu(\eta x(t) + y(t)) + \mu_h \eta_h y_h(t)] - w_h(t)}{\rho} - \gamma_h y_h(t) \tag{6.9}$$

Again, to study the steady-state behavior, we set (6.6) – (6.9) to zero and solve for the steady-state average number of peers (x), seeders (y), helpers (x_h), and microseeders (y_h) numerically. The download time is now given by

$$T_{\mathrm{dl}} = \frac{1}{\frac{\varepsilon[\mu(\eta x + y) + \mu_h \eta_h y_h]}{x}}. \tag{6.10}$$

In the next section we show numerical solutions obtained from this analysis for different simulation setups along with results that demonstrate the accuracy of the first-order fluid-model analysis.

6.2.4 Evaluations

We have implemented a discrete-time packet-level simulator to simulate a BitTorrent file sharing system. In this system, leechers follow the BitTorrent protocol exactly and helpers follow the proposed helper protocol, which is backwards-compatible with the BitTorrent protocol. Among other things, the simulator explicitly implements the most important features of the file sharing system/protocol, namely:

- Accounting for individual pieces of a file;
- Accounting for peer activities such as arrivals, aborts, departures, piece uploads and piece downloads;
- Local-rarest-first piece selection;
- Tit-for-tat policy in conjunction with choking/unchoking (including optimistic unchoking);
- Accounting for bandwidths of network links.

We first study the accuracy of the fluid model by comparing the average download time computed using the fluid model to that obtained from simulations. We use two different setups. Setup 1 mimics a relatively small file with a small-sized swarm while Setup 2 has a large file with a medium-sized swarm. The parameters for the 2 setups are shown in Table 6.1. Under each setup, we simulated the system with and without helpers.

	Setup 1	Setup 2
λ(peer/s)	0.2	0.2
θ(1/s)	0.000625	0.0000625
μ(Kbps)	512	512
c(Kbps)	2048	2048
γ(1/s)	0.0025	0.00025
λ_h(peer/s)	0.05	0.1
θ_h(1/s)	0.00125	0.00025
μ_h(Kbps)	512	512
c_h(Kbps)	2048	2048
file size (MB)	100 ($N = 400$ pieces)	1000 ($N = 1000$ pieces)
k	8	10

Table 6.1: Parameters of 2 different setups for helper-assisted BitTorrent-compatible peer-to-peer file download.

Table 6.2 shows that under both setups, whether there are helpers or not, the average download time, the number of leechers, and the number of seeders in the system in steady state are all accurately estimated by the fluid model.

The fact that the fluid-model analysis results closely match the simulation results has the following implications. First, the assumption that peers' upload bandwidths are fulled utilized is valid. Indeed, Figure 6.1 plots the system throughput and the total amount of upload bandwidth in the system under Setup 1. We can see

Setup 1	Helper	DL time	# of peers	# of seeds
Model	No	1344.83	181.924	34.519
Model	Yes	1090.24	158.11	40.47
Simulation	No	1389.29	187.15	35.23
Simulation	Yes	1161.02	163.30	39.29

(a)

Setup 2	Helper	DL time	# of peers	# of seeds
Model	No	13448.3	1819.24	345.19
Model	Yes	10902.4	1581.1	404.726
Simulation	No	13551.7	1829.52	350.03
Simulation	Yes	11309.7	1622.74	393.30

(b)

Table 6.2: The average download time, number of leechers, and number of seeders obtained through the fluid-model analysis all match closely with simulation results under both setups, with or without helpers.

that the system throughput is extremely close to the total available upload bandwidth, indicating that leechers', seeder' and helpers' upload bandwidths are all very close to being fully utilized. It is consistent with our earlier analysis that even if helpers only download a fixed small number of pieces (in this case $k = 8$ out of 400), they can still efficiently utilize their upload bandwidth. Second, it confirms that the number of pieces helpers need to download to fully utilize their upload bandwidth needs not scale with the file size. In Setup 2, helpers only download 10 out of 4000 pieces of a file and yet the simulation result matched the fluid-model result. This can only happen if the assumption that peers' upload bandwidth is fulled utilized is valid.

We empirically study the effect of the number of pieces helpers download. Figure 6.2 plots the average leecher download time versus the number of pieces helpers download (k). $k = 0$ is equivalent to a system with no helpers. We see that as k first increases, the average leecher download time decreases. This is because if

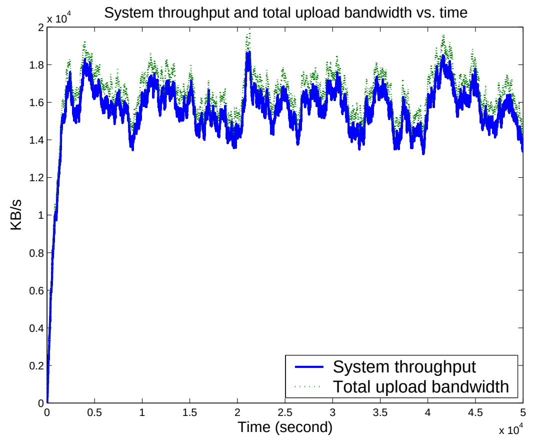

Figure 6.1: Throughput and total upload bandwidth of the system over time. System throughput is very close to total upload bandwidth, indicating that leechers', seeder' and helpers' upload bandwidths are all very close to being fully utilized.

k is too small, the probability that a helper is useful to a randomly selected peer, as computed in Section 6.2.2, is not high enough to offset the associated connection time and query overhead of helpers. However, after the leecher download time hits a low point, the leecher download time increases as k increases. This is because once helpers obtain enough pieces to fully utilize their upload bandwidth, downloading more pieces will only waste system resources. This result explains why the methods in [49] and [35] are suboptimal.

Figure 6.3 shows the CDF of leecher download time of three different systems under Setup 1:

1. An upper-bounding setup where helpers join the download session with $k = 8$ random pieces preloaded;

2. A system with regular helpers;

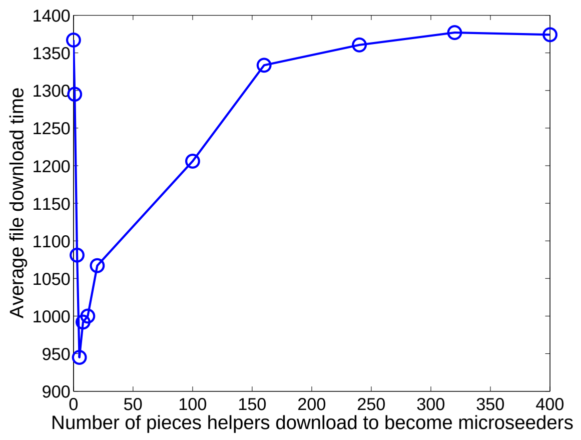

Figure 6.2: Average leecher download time vs. number of pieces (k) helpers download. As k increases from 0, there is a drastic drop in the average leecher download time as the helpers become able to contribute their upload bandwidth. But as k further increases, there is a gradual increase in average leecher download time. This is consistent with the fluid-model analysis.

3. An unaltered BitTorrent system.

The comparison between System 2 and 3 shows that leechers in a system with helpers have a much lower average download time. The comparison between System 2 and 1 shows that there is very little difference in system performance whether the helpers need to download k pieces from the system or not. In other words, helpers' consumption of system resources is negligible and yet their upload bandwidth can be fully utilized.

Finally, we present results with heterogenous peers. We simulated three classes of users with different upload/download bandwidths. Notation wise, we use a:b Kbps to denote that the user has a Kbps download bandwidth and b Kbps upload bandwidth. Among all the peers, 25% of them belong to the slow class,

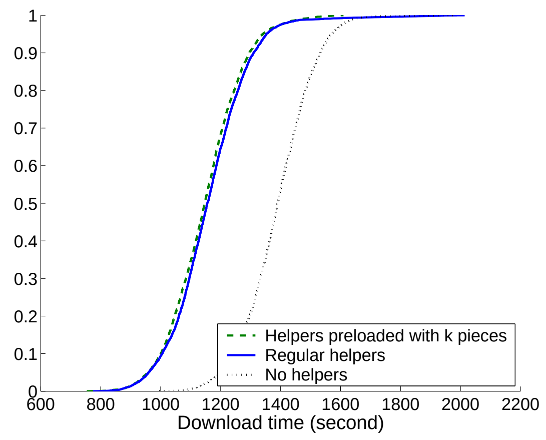

Figure 6.3: CDF of leecher download time in three different systems. System 1: an upper-bounding setup in which helpers join the swarm with $k = 8$ random pieces preloaded. System 2: system with regular helpers. System 3: an unaltered BitTorrent system. It shows that helpers are very effective in reducing leechers' average download time and the amount of resources helpers consume is negligible.

with 512:128 Kbps bandwidth. 50% of the them belong to the middle class with 2048:512 Kbps. The other 25% belong to the fast class with 8:1 Mbps. 75% helpers have 2048:512 Kbps and the rest have 8:1 Mbps. The rest of the parameters are the same as in Setup 1. Figure 6.4 plots the CDF of file download time for each class of leechers. It shows that helpers reduce the download time for all the leechers, but are most helpful to leechers with slower upload/download speed. This is because due to BitTorrent's optimistic unchoking policy, from empirical studies, peers with similar upload capacities tend to become each other's active neighbors. As a result, peers with smaller upload capacities tend to get a smaller proportion of the total upload bandwidth of the system than their population.[5] Consequently, even with the same

[5]This behavior is unfortunately very difficult to capture analytically. Thus we do not incorporate it in the fluid-level analysis.

arrival rate, there are more slow peers in the system than fast peers. Since helpers do not discriminate between slow and faster peers, a larger fraction of helpers' bandwidth is naturally used to help the slow peers. Further, slow peers are downloading at a lower rate than fast peers, thus with the same amount of additional bandwidth, the slow peers will get a bigger percentage reduction in average download time than the fast peers.

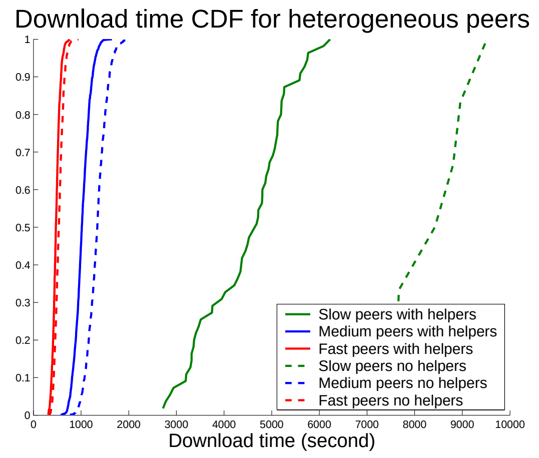

Figure 6.4: CDF of peer download time for users with different upload/download bandwidths. All the leechers can benefit from helpers but the leechers with the smallest upload bandwidth enjoy the most noticeable reduction in average download time.

Finally, we would like to point out that if the helpers spend too little time in the system and spend most of it downloading the required number of pieces, the overall system performance could actually be hurt.[6] However, since the number of pieces helpers download is extremely small, this case rarely occurs in practice. Also,

[6]Note that it is the total amount of time they spend in the system that matters. The system performance will not be adversely affected even if the helpers log on and off frequently, but preserve the small number of pieces they have downloaded across sessions.

when there are enough helpers in the system to fill up leechers' download pipes, any more helpers will not help with system performance. Thus the tracker may use the fluid model analysis as a guideline to turn away helpers when the helper arrival rate exceeds the rate required to fill up leechers' download pipes.

6.3 Extension to live video multicast

In this section, we extend the usage of helpers to a different but important class of video distribution: live multicast. Examples include TV-over-Internet and live sports broadcast. Compared to file download, live video multicast has the following defining characteristics:

1. Peers in the system have synchronized playback time;
2. Each packet has a specific delivery deadline;
3. The streaming content is constantly updated.

These characteristics make efficient utilization of helpers even more crucial. As the streaming content constantly changes, helpers must be constantly downloading in order to be constantly uploading. Like in the download case, helpers have to upload more than they download to contribute to the system. Further, helpers must distribute packets to meet specific delivery deadlines.

We consider a hybrid system in which the content server will supplement the extra bandwidth that peers are not able to obtain from each other. The main performance metric of such a system is the required server bandwidth given the same startup delay and buffer length. In such a system, if the video bit rate is lower than the average peer upload bandwidth, the system can be maintained with very little server bandwidth [32, 41]. However, if that is not the case, the server bandwidth will increase linearly with the number of peers in the system, which is not scalable. Our goal is to optimally utilize helpers' upload capacity in order to provide video streaming at rate beyond peers' average upload bandwidth without incurring additional server load.

6.3.1 Design guideline

One equivalent way of formulating our problem is to maximize peers' streaming rate R given a fixed set of peers, helpers, and server load. We use a first-order fluid-level analysis to guide the system design. Recall that in Section 6.2.3, we also use a fluid-level analysis and establish equations regarding the rates at which the numbers of each type of peers change. Here we take a snapshot of the system and use the following simple relationship to derive a performance upper bound. At any point of time,

total system upload bandwidth $\geq$ sum of peers' downloading rate.

Let P and H denote the set of peers and helpers in the system respectively. $|P|$ and $|H|$ are the numbers of peers and helpers respectively. Let u_i be the upload bandwidth of Peer i and u_j^H be the upload bandwidth of Helper j. Let S_P and S_H denote the fixed total bandwidth server allocates to peers and helpers respectively. Let $R_{P \to P}$ denote the total traffic among peers and $R_{H \to H}$ denote the total traffic among helpers. Similarly, let $R_{P \to H}$ denote the total traffic from peers to helpers and $R_{H \to P}$ denote the total traffic from helpers to peers. R_i^H denotes the rate Helper i receives.

The total rates that peers and helpers receive are

$$|P|R = S_P + R_{P\to P} + R_{H\to P}, \text{ and} \tag{6.11}$$

$$\sum_{i\in H} R_i^H = S_H + R_{H\to H} + R_{P\to H} \text{ respectively.} \tag{6.12}$$

The system throughput has to be smaller than or equal to the total available upload bandwidth. Therefore

$$R_{H\to H} + R_{P\to H} + R_{P\to P} + R_{H\to P} \le \sum_{i\in P} u_i + \sum_{i\in H} u_i^H. \tag{6.13}$$

Combining (6.11), (6.12) and (6.13) yields

$$R \le \frac{S_H + S_P + \sum_{i\in P} u_i + \sum_{i\in H} u_i^H - \sum_{i\in H} R_i^H}{|P|}. \tag{6.14}$$

To maximize R, we need to minimize $\sum_{i\in H} R_i^H$ while keeping both peers and helpers fully utilizing their upload capacity. In practice, R_i^H cannot be made arbitrarily small for two reasons. Firstly, video data is broken into packets and transmitted. The packets cannot be too small in size in order to reduce transmission overhead. Let us conceptualize video as being broken into short segments, each m seconds long. Each segment consists of k packets of equal sizes. Then for a helper to be useful to peers downloading a particular segment, the least it has to download is one packet. As peers move forward in playback time constantly, helpers have to download at least 1 packet out of every segment (k packets). Therefore, $R_i^H \ge \frac{R}{k}$ and $\sum_{i\in H} R_i^H \ge \frac{|H|R}{k}$. Secondly, R_i^H caps the rate at which Helper i can upload to any one peer. Thus, for Helper i to fully utilize its upload bandwidth, it has to constantly have $\frac{u_i^H}{R_i^H}$ peers to upload to, which cannot be maintained if R_i^H is too small.

To summarize, we have

$$R \leq \frac{S_H + S_P + \sum_{i \in P} u_i + \sum_{i \in H} u_i^H}{|P| + \frac{|H|}{k}}, \tag{6.15}$$

where equality holds if each helper downloads only 1 packet out of every k packets of a segment, and all the peers and helpers in the system can fully utilize their upload bandwidth.

While it has been shown in previous works, e.g. [33, 53], that peers can very efficiently utilize their upload bandwidth in video streaming over P2P overlay networks, we need helpers to also fully utilize their upload bandwidth even if they only have 1 packet out of every k packet. In a highly dynamic environment, if each helper carries one random uncoded data packet for each segment, it can be difficult for helpers to be consistently connected to enough peers that are missing the particular packets they are carrying, especially for unstructured overlay networks. As a result, helpers either have unused upload bandwidth or waste a lot of resources establishing connections. Instead, we propose a system in which peer helper carries one MDS erasure coded packet of each segment. Figure 6.5 illustrates the proposed solution. The content server breaks each segment of video into k packets and generates $n - k$ parity packets using an (n, k) systematic MDS erasure code. The server uploads the k data packets to the peers at rate $S_P \geq R$. Helpers break into $n - k$ clusters with approximately the same total upload bandwidth. Every m seconds (the length of a segment), the server uploads 1 unique parity packet to each helper cluster at total rate $S_H = \frac{R(n-k)}{k}$. Each cluster of helpers circulate among themselves one and only one parity packet, i.e. $R_j^H = \frac{R}{k}$, $\forall j$. Each peer maintains connection to each cluster and requests parity packets when needed.

If the average upload bandwidth of peers is $\frac{\sum_{i \in P} u_i}{|P|} = \alpha R$ $(\alpha < 1)$, then on average, peers miss $(1-\alpha)k$ packets out of every k packets of a segment. This requires that the helpers have at least αk unique parity packets, i.e. $n-k \geq \alpha k = \frac{k\sum_{i\in P} u_i}{|P|}$. Peers can miss at most k packets in each segment therefore $n-k \leq k$. However, since S_H does not scale with the number of helpers or the number of peers, it is beneficial to pick $n-k=k$ such that the helper clusters can potentially accommodate the entire packet drop range.

In addition to ease of finding peers to upload to, there are other benefits to having helpers carry parity packets instead of random uncoded data packets. Depending on the explicit implementation of the P2P overlay and the packet exchange strategy, there may be particular packets that a lot of peers are missing due to peer churning or link congestion. It is also difficult to predict which packet(s) will be in such demand. If the helpers carry uncoded packets, some helpers will be overstressed while others will have spare capacity. This effect is mitigated if helpers carry coded packets. In short, we would like each helper to be equally useful to all peers to facilitate full utilization of helpers' upload bandwidth. This is also why we would like to keep the available upload bandwidth of each helper cluster approximately the same. We will demonstrate through simulations that the proposed system is one of the constructive solutions that can approach the equality in (6.15) very closely.

6.3.2 Rate allocation

As stated earlier, for equality to hold in (6.15), we need both peers and helpers to be fully utilizing their upload bandwidth. In a P2P system, each peer connects to multiple other peers (neighbors) simultaneously. Compared to download capacity, peers' upload capacity is limited and oftentimes the most prominent con-

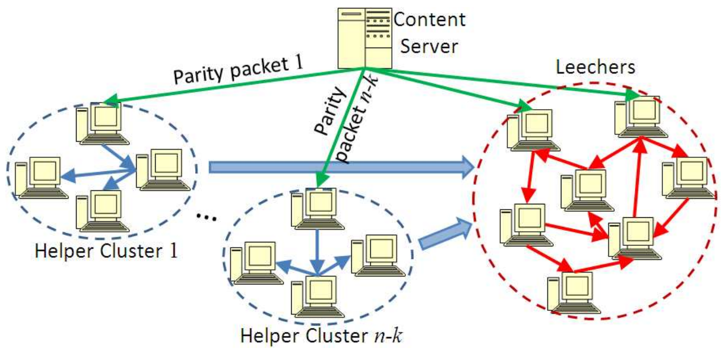

Figure 6.5: Proposed hybrid peer-to-peer video multicast system with helpers.

straint of such systems as peers are often connected via DSL and cable modem (even fiber optic service hosts have very asymmetric access). When multiple connections contend for the limited upload capacity, the natural contention will result in (say via TCP congestion control) an implicit rate allocation, in which the upload capacity is evenly divided among all the connections as empirically observed in [13]. However, this simple scheme does not always result in optimal utilization of peers' upload bandwidth.

In this section, we formulate a convex optimization problem that minimizes server bandwidth and provides a distributed optimization solution. We then propose a light-weight rate allocation protocol that mimics the distributed optimization solution and dictates how much bandwidth to allocate to each connection. Through extensive simulations, we show that the proposed rate allocation allows the participating peers to fully utilize their upload bandwidth and minimize server bandwidth, with or without helpers.

Notations and assumptions

Suppose there are n peers in the system at any instant of time. Denote them as Peer k ($k = 1, 2, ..., n$). When Peer j arrives, it connects to a subset of peers already in the system (say including Peer i) and requests data from them. $x_{i,j}$ is the rate Peer i allocates from its upload capacity u_i to serve Peer j. Each peer keeps track of its total upload capacity, which can initially be estimated based on historical values and then measured/updated once data starts to flow to its neighbors. N_j denotes the set of all peers connected to Peer j (Peer j's neighbors). The aggregate rate Peer j receives from all of its neighbors is denoted as $x_j = \sum_{i \in N_j} x_{i,j}$. Denote R as the video bitrate. R is also Peer j's desired streaming rate in order to maintain smooth video playback. It is clear that smooth video playback requires $x_j \geq= R$. If $x_j < R$, Peer j will request data from the server at rate $R - x_j$ to make up for the deficit. The aggregate rate at which Peer i uploads to all its neighbors is $\sum_{j \in N_i} x_{i,j}$. Clearly, this cannot exceed Peer i's upload bandwidth, i.e., $\sum_{j \in N_i} x_{i,j} \leq u_i$. Furthermore, for unified representation, we denote the server as Peer 0. Thus, $x_{0,j}$ is the rate Peer j obtains from the server, which satisfies $x_{0,j} = \max(0, R - x_j)$.

In the analysis, we assume that a peer (say Peer A) can upload to another peer (say Peer B) as fast as they want within its upload capacity. In practice, the speed at which Peer A can upload to Peer B is also determined by how much content is needed by Peer B from Peer A. This assumption is automatically removed in the packet-level simulation.

Optimization framework

The most straightforward formulation of minimizing the server load using an optimization framework is the following:

$$\min \sum_j \max(0, R - \sum_{i \in N_j} x_{i,j}) \tag{6.16}$$

$$\text{s.t.} \sum_{j \in N_i} x_{i,j} \le u_i \ \forall\ i \neq 0, \ \text{and} \tag{6.17}$$

$$x_{i,j} \ge 0 \ \forall\ i, j. \tag{6.18}$$

We introduce a utility function $f(\cdot)$ for each peer in terms of the aggregate rate received from all its neighbors (excluding the server or Peer 0). We show that if $f(\cdot)$ is monotonically increasing, differentiable everywhere and strictly concave, the solution to maximizing the total system utility will also minimize server load. This optimization problem bears a distributed solution that is suitable for large scale P2P systems.

Proposition 2. *If $f(\cdot)$ is monotonically increasing and strictly concave, solutions to*

$$\max \sum_j f(\sum_{i \in N_j} x_{i,j}) \tag{6.19}$$

$$s.t. \sum_{j \in N_i} x_{i,j} \le u_i \ \forall\ i \neq 0, \ \textit{and} \tag{6.20}$$

$$x_{i,j} \ge 0 \ \forall\ i, j. \tag{6.21}$$

are a subset of solutions to (6.16) and hence minimize server load.

Proof. Because $f(\cdot)$ is monotonically increasing, it is easy to show through contradiction that when $\sum_j f(x_j)$ is maximized, $\sum_{j \in N_i} x_{i,j} = u_i \ \forall\ i$.

Since $f(\cdot)$ is strictly concave in $x_{i,j}$ and monotonically increasing, $\sum_{j\in N_i} x_{i,j} - u_i$ is concave in $x_{i,j}$, $\sum_{j\in N_i} x_{i,j} = u_i \; \forall \; i$, the necessary and sufficient conditions for (6.19) are:

$$\frac{d}{dx_{i,j}} f(\sum_{i\in N_j} x_{i,j}) - \mu_i + \gamma_{i,j} = 0 \; \forall \; j, \tag{6.22}$$

$$\mu_i > 0 \; \forall \; i, \tag{6.23}$$

$$\gamma_{i,j} \geq 0 \; \forall \; i, j, \tag{6.24}$$

$$\gamma_{i,j} x_{i,j} = 0 \; \forall \; i, j. \tag{6.25}$$

For these necessary and sufficient conditions to be satisfied, for Peer i, either $x_{i,j} = 0$, or $\frac{d}{dx_{i,j}} f(\sum_{i\in\{0,N_j\}} x_{i,j}) = \mu_i \; \forall \; j \in N_i$.

Since (6.16) has the exact same constraints as (6.19), it is easy to show that any solution that satisfies the necessary and sufficient conditions of (6.19) will also satisfy the sufficient conditions for (6.16). Hence any solution for (6.19) is also a solution to (6.16). $\square$

Distributed solution

One important characteristic of (6.19) is that the constraints are local in that the rate assignment $x_{i,j}$ is constrained locally at Peer i, i.e. $x_{i,j} \geq 0$ and $\sum_{j\in N_i} x_{i,j} \leq u_i$. This allows us to use a classical iterative algorithm for convex optimization and directly obtain a distributed solution to (6.19) [11].

Specifically, we adopt the gradient projection algorithm. At Peer i, $x_{i,j}$ is initialized to $\frac{u_i}{|N_i|}$ for $j \in N_i$ and 0 otherwise, where $|N_i|$ is the number of neighbors Peer i has. $x_{i,j}$ is updated at each step as follows:

$$\dot{x}_{i,j} = \Delta \cdot \frac{\partial}{\partial x_{i,j}} f(\sum_{i \in N_j} x_{i,j}), \tag{6.26}$$

$$x_{i,j} = [x_{i,j} + \dot{x}_{i,j}]^{+} \tag{6.27}$$

where $[\cdot]^{+}$ denotes l_2 projection onto a feasible set.

With the constraints on $x_{i,j}$, the objective function in (6.19) satisfies Lipschitz condition. Thus, by carefully choosing the update step size Δ, convergence can be guaranteed [11].

Here we propose a light-weight heuristic based protocol that mimics this optimization solution. The essence of the solution is that Peer i slowly adjusts the rate at which it uploads to its neighbors such that its neighbors' aggregate received bandwidth is the same, i.e. $\frac{d}{dx_{i,j}} f(\sum_{i \in \{0,N_j\}} x_{i,j}) = \mu_i \; \forall \; j \in N_i$. Since a peer's buffer level is a good reflection of its aggregate received bandwidth, we try to equalize each peer's neighbors' buffer levels by having peers upload the next packet to the neighbor with the lowest buffer level.

We will detail the system description and discuss the complexity of this protocol in the following section. We will then demonstrate the effectiveness of this rate allocation scheme in Section 6.3.4.

6.3.3 System description

With these design guidelines in mind, we now present the proposed system in detail. Before describing how the helpers function, we first describe the peer network for the sake of completeness. The peer network we use is an unstructured mesh-based overlay network similar to [33] and [53]. We choose to use an unstructured overlay to reduce network maintenance overhead, which is essential in high-churn applications like live video streaming. However, the proposed helper system will work with a structured tree (or multi-tree) based peer overlay network as well.

Peer network

Overlay network formation and maintenance: The content provider owns a source node (content server) that connects to a small number of peers (20 in our case). Similar to BitTorrent, the content provider also maintains another server, called *tracker*, to keep track of all the peers in the streaming session and to assist building the overlay network[7]. A joining peer first queries the tracker to obtain a list of peers and synchronize with system clock. It then contacts these peers to establish connections with them. Each peer is allowed a maximum number of neighbors, which is proportional to its upload bandwidth. A peer will reject a new connection request if it already has enough neighbors. If the number of neighbors connected to a peer falls below a threshold, the peer will contact the tracker to obtain a new list of peers to connect to. In our implementation, when the tracker is queried for a list of peers, it chooses randomly among the existing peers. This may result in an inefficient overlay network. To improve the quality of the network, we adopt a neighbor-pruning method similar to the one described in [53]. Specifically, each peer periodically (every 5 seconds in our case) checks the throughput between itself and each of its neighbors. If the throughput is below a certain threshold, it will disconnect from that neighbor. This method has shown to greatly improve the system throughput of a practical system [53].

[7]Tracker can also be distributed using distributed hash table techniques.

Peer packet exchange protocol: The source node generates new packets with monotonically increasing ID's in real-time. Like in [33], each peer maintains a window of interest, which is the range of packets that it is interested in obtaining. Each peer also maintains a window of availability, which is the range of packets that it is willing to share with its neighbors. Peers exchange packets by updating each other with availability maps and using a pull-based packet request protocol. We assume each second of video consists of an integer number of GOPs and k equal sized packets packets. Peer move both their window of interest and window of availability forward once every one-second. Note that this interval is correlated with the maximum startup delay of the system. The longer this interval, the longer the startup delay. This is because before the peers can slide their windows forward for the first time, they need to first fill up their window of interest to that amount.

To choose which packet to request from each neighbor, peers follow a BitTorrent-like local-rarest-first strategy within its window of interest and requests the packet that is the rarest within its one-hop neighborhood. Naturally, a peer may have multiple requests pending. In choosing which request to fulfill first, as discussed in Section 6.3.2, instead of choosing randomly or following a round-robin fashion, peers first satisfy the request from a neighbor who possesses the fewest number of packets in its window of interest. Intuitively, this strategy works because a peer's upload bandwidth can only be utilized if it has packets that other peers need. Thus if a peer has too few packets in its buffer, it may not be able to fully utilize its upload bandwidth. On the other hand, if a peer already has a lot of packets, it most likely already has a lot of pending requests. Since its upload bandwidth is limited, it cannot satisfy all these requests even if it gets more packets. Therefore, in terms of increasing system throughput, it isn't as meaningful to fulfill the request of a peer that already has a lot of packets.

In the analysis in Section 6.3.2, we assume that Peer i can upload to Peer j at rate $x_{i,j}$ as long as the upload bandwidth constraint is not violated. In practice, $x_{i,j}$ cannot be realized unless Peer i has sufficient content that Peer j needs. Therefore we build the topology such that peers with more upload bandwidth have more neighbors. Given the same number of packets in the buffer, peers with more upload bandwidth get more packet requests and can thus still fully utilize their upload bandwidth. This greatly reduces the need to have a sophisticated algorithm that also takes peers' upload bandwidth into consideration. The information regarding the fullness of a peer's window of interest can be easily piggy-backed in the packet request with marginal overhead.

Like in [33], the content server also implements request overriding at the source. Specifically, the content source, or server, maintains a list of packets that have never been uploaded before. If the list is not empty and the server receives a request for a packet that is not on the list, the server will ignore the packet request, send the oldest packet on the list instead, and delete that packet from the list. This algorithm ensures that at least one copy of every packet is uploaded quickly, and the server will not spend its upload bandwidth on uploading packets that could be obtained from other peers unless it has spare bandwidth available.

As we show shortly in the Section 6.3.4, the resulting video streaming overlay network is quite efficient, utilizing more than 97% of peers' available bandwidth.

Helper network

As mentioned earlier, the rate that the content server allocates helpers is $S_H = \frac{R(n-k)}{k}$, which does not scale with the number of helpers or peers. Thus, we choose $n = 2k$. The content owner applies a $(2k, k)$ systematic MDS erasure code over each second of video data and generate k distinct parity packets for the k helper clusters. Ideally, we would like each of the helper cluster to have the same amount of spare upload bandwidth. To approximate this, the tracker keeps track of the total amount of upload bandwidth of each helper cluster. As a new helper joins the network, it reports to trackers its estimated upload bandwidth. The tracker then assigns it to the helper cluster with the least amount of available upload bandwidth. For instance, let Helper i have upload bandwidth u_i. The amount of bandwidth it can contribute to the system is then $u_i - R/k$. If a cluster has N helpers, the total available upload bandwidth is then $(\sum_{i=1}^{i=N} u_i) - \frac{NR}{k}$. In practice, helpers' upload bandwidth may fluctuate and they can update the tracker when needed.

Each cluster of helpers will form their own overlay network and exchange packets with each other using the exact same mechanism as regular peers. To further facilitate full utilization helpers' upload bandwidth, we have the helpers download content 1 second ahead of peers. For example, if the current time is 14 second and the buffer length is 5 second, then the peers share data packets up to the 9th second and the helpers share parity packets up to the 10th second. This way, peers can download from helpers without having to wait for them to finish downloading the parities first.

Interaction between peers and helpers

As a peer joins, it also queries the tracker for a list of helpers. Each peer maintains connections to at least one helper from each of the $n - k = k$ clusters. Each helper is allowed a maximum number of peer neighbors that is proportional to its upload bandwidth. Peers periodically prune helpers that consistently fail to provide the requested packets in time.

Helpers inform all their neighbors (both peers and helpers) every time they receive a new packet. As they receive only one new packet per second on average, the overhead is small.

In deciding what to request from helpers, peers partition their window of interest into two parts: urgent and regular. The urgent part of the buffer is the part that is close to being shifted out of the downloading buffer for processing and playback. Suppose it is of length u second. A peer will always request parity packets for the urgent part first if it has not started receiving uk distinct packets in that interval. It will also flag the request control message as urgent. For the regular buffer zone, peers request parity packets in a local-rarest-first manner. In our implementation, the urgent zone is one second long. In general, the urgent zone length can be any integer multiple of the window-sliding interval.

Helpers use the following rules to decide which request to satisfy first. Helpers will always satisfy requests from other helpers first, as this will enable other helpers to contribute their upload bandwidth. Among peers' requests, helpers will always satisfy the urgent requests first. For the regular requests from peers, helpers will first satisfy the peers whose buffer levels are the lowest to mimic the distributed optimization solution.

6.3.4 Simulation results

We evaluate the performance of the proposed system through a discrete-time packet-level simulator. The simulator implements the most important components of the system including: (i) accounting for individual packets of video data (we use $n = 40$, $k = 20$ per second of video.); (ii) peer activities such as arrivals, departures, packet uploads and downloads; (iii) packet request algorithm; (iv) overlay network maintenance and (v) bandwidth constraints of peers. The downloading buffer keeps 10 seconds' data and the startup delay is 3 seconds.[8] All the tests are 500 seconds long.

We first present simulation results with non-churning heterogeneous peers to demonstrate that both peers' and helpers' upload bandwidth can be efficiently utilized using the proposed system and the number of helpers needed can be reasonably estimated using the simple computation in (6.15). All the peers (including helpers) have unlimited download bandwidth and the following upload bandwidth distribution: 40% of them have 384 Kbps upload bandwidth, 40% have 512 Kbps and the other 20% have 768 Kbps. The average upload bandwidth of peers is 512 Kbps. The number of peers in the system is 2000. Peers enter the system at Time 0 and stay until the end, as do helpers. We plot the bandwidth needed from the server as a percentage of total bandwidth consumed by peers watching the video. The dashed line is the result computed from the simple fluid-level analysis whereas the solid line was obtained through simulation. When there are no helpers in the system, the bandwidth shortage is just slightly above 20%. This is expected since peers' average upload bandwidth is 20% less than video bitrate. This also indicates the peer net-

[8] Upon joining, video will start playing after exactly 3 seconds. Peers fetch from the server if needed to start playing by the end of 3 seconds.

work is very efficient on its own, utilizing 97.81% of peers' upload bandwidth. Using (6.15), 533.33 helpers are needed to reduce server load to zero. In our simultion, with 533 helpers in the system, the server load can be reduced to 2.40% of the total rate needed by peers. An additional 67 helpers can further reduce server load to 0.7% of the total rate. As predicted by the analysis, server load decreases linearly as the number of helpers increases. This result demonstrates that (6.15) can serve as a good estimate of system performance. We can use it to estimate the server load given a video bit rate and a certain number of peers and helpers or estimate the number of helpers needed to bring the server load down to a desired level.

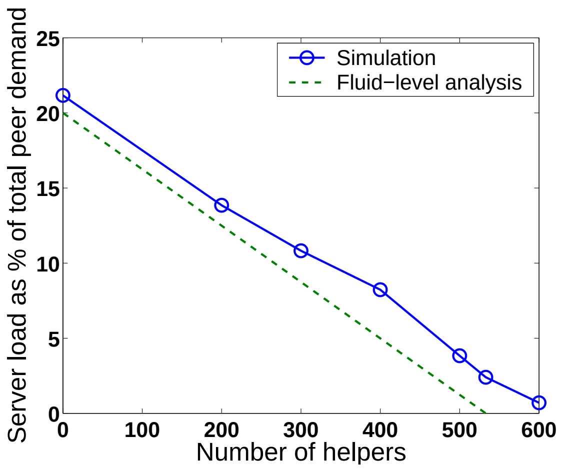

Figure 6.6: Average server load with different number of helpers. We also plot the server load computed by the simple fluid-level analysis. The two curves are fairly close, indicating that the fluid-level analysis serves as a good estimate of system performance. Server load decreases linearly as the number of helpers increases.

We then simulate peer churning by having peers follow a Poisson arrival process and exponentially distributed staying time. The bandwidth distribution of peers remains the same as before. In this test, peers arrive at 2 peers/second on average with an average staying time of 1000 second. In steady state, there are 2000 peers in the system on average. Helpers' average staying time is 500 second. We vary helpers' arrival rate to adjust the number of helpers in the system in steady state. For example, for the system to have 500 helpers on average, the helper arrival rate is 1 per second. For the system to have 600 helpers on average, the helper arrival rate is 1.2 per second. In Fig. 6.7, we plot the average server load vs. the average number of helpers and compare the result to when the peers are static, i.e. all of them join at Time 0 and stay until the end as in the previous experiment. We see that peer churning only creates a very mild increase in server load. Nonetheless, the server load decreases linearly as the number of helpers increases as predicted by (6.15). This experiment shows that the proposed system is effective with churning peers and regardless of the number of helpers in the system.

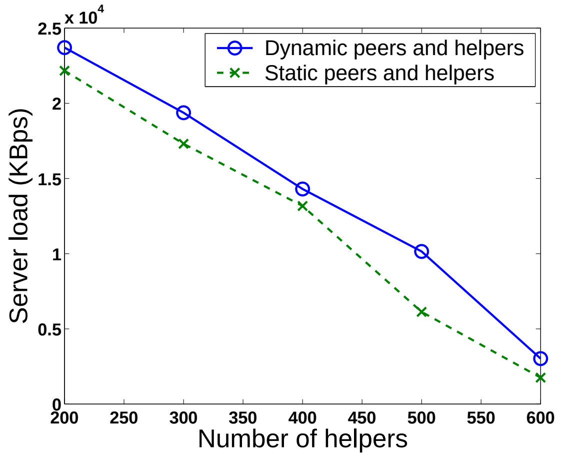

Figure 6.7: Comparison of average server load when the peers (including helpers) are dynamic vs. when peers are static. There is only a small increase in server load when peers are dynamic.

Finally, we demonstrate that the proposed system is robust to highly dynamic helpers as well. We vary the helper arrival rate from static (helpers join at Time 0 and stay until the end) to 6 helpers per second (helpers follow a Poisson arrival process with an exponential staying time). We keep the average number of helpers in the system to be 600 in steady state. The higher the helper arrival rate is, the shorter the average helper staying time is. Figure 6.8 shows that as we increase the helper churning rate, there is no significant increase in server load and the increase does not scale with the helper arrival rate. This indicates that the proposed system is very robust to highly dynamic network topology and peer activities.

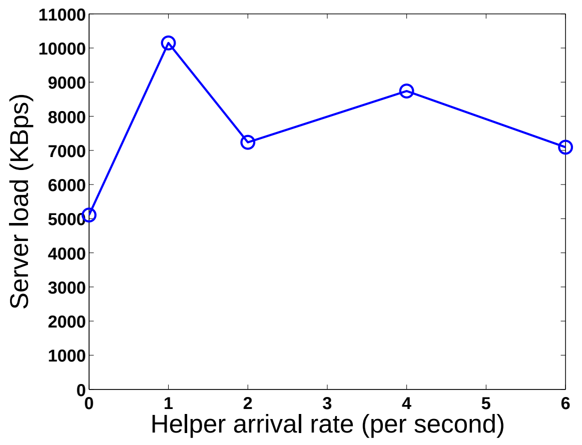

Figure 6.8: Server load under different peer arrival rates. The average number of peers in the system is kept at 2000. Higher peer arrival rate implies lower peer staying time. As the peer churning rate increases, there is no significant increase in server load.

Chapter 7

Conclusion and future work

In this part of the thesis, we studied enhancing performance of video distribution over uplink-scarce peer-to-peer networks by optimally utilizing helper peers' upload bandwidths. It is important to understand that higher system throughput does not necessarily lead to better system performance. This is because while helpers can increase system throughput by contributing their upload bandwidth, they also need to consume system resource before they become useful. We have developed light-weight and distributed helper protocols for both video file download and live multicast such that helpers can maximally contribute their upload bandwidth while minimally consuming system resources. We have analyzed system performances using first-order analysis and cross-verified through extensive simulations. Our simulation results demonstrate that helpers can indeed almost fully contribute their upload bandwidth and improve system performances.

Along this line of work, there are numerous promising directions for future research.

- For file download, it would be interesting to analyze system performance under arbitrary peer arrival and departure processes.

- We would like to extend the usage of helper to video-on-demand streaming. While there exist simple strategies that work well, finding the optimal usage of helpers is challenging due to the unique attributes of asynchronous playback times and the possibility of downloading ahead of playback point in VoD systems.

- Optimal usage of helpers across different P2P sessions is an interesting topic. Specifically, we are interested in developing a distributed solution. The goal is to have helpers independently determine which session or sessions or join with minimal interaction with central servers.

- Incentive, especially incentive with shared memory, for all P2P systems remains an active area of research and an open question in general.

We believe the P2P framework is a useful tool to enable high-quality Internet video that can scale gracefully to millions of viewers. In this thesis, we have only touched a tip of the iceberg. We hope the philosophy of this work can provided some ideas and intuitions to researchers in this area.

Bibliography

[1] [Online]. Available: http://dss.clip2.com/GnutellaProtocol04.pdf

[2] "KaZaA." [Online]. Available: http://www.kazaa.com

[3] "SETI@home." [Online]. Available: http://setiathome.ssl.berkeley.edu/

[4] "Skype." [Online]. Available: http://www.skype.com

[5] "Global Internet Geography 2006," *TeleGeography Research*, 2006.

[6] A. Amraoui and R. Urbanke, "Ldpcopt," 2003. [Online]. Available: http://lthcwww.epfl.ch/research/ldpcopt/bschelp.php

[7] X. Artigas, J. Ascenso, M. Dalai, S. Klomp, D. Kubasov, and M. Ouaret, "The DISCOVER Codec: Architecture, Techniques and Evaluation," *Proc. Picture Coding Symposium*, 2007.

[8] A. Ashikhmin, G. Kramer, and S. Brink, "Extrinsic information transfer functions: model and erasure channel properties," *IEEE Trans. Information Theory*, vol. 50, pp. 2657–2673, Nov 2004.

[9] S. Battista, F. Casalino, and C. Lande, "MPEG-4: A Multimedia Standard for the Third Millennium. 1," *IEEE Multimedia*, October-December 1999.

[10] ——, "MPEG-4: A Multimedia Standard for the Third Millennium. 2," *IEEE Multimedia*, January-March 2000.

[11] D. Bertsekas and J. Tsitsiklis, *Parallel and Distributed Computation.* Old Tappan, NJ (USA); Prentice Hall Inc., 1989.

[12] N.-M. Cheung and A. Ortega, "Compression Algorithms for Flexible Video Decoding," in *Proceedings of Visual Communications and Image Processing*, Jan. 2008.

[13] D. Choffnes and F. Bsutamante, "Taming the Torrent: A Practical Approach to Reducing Cross-ISP Traffic in Peer-to-Peer Systems," in *Proceedings of ACM SIGCOMM*, 2008.

[14] B. Cohen, "Incentives build robustness in BitTorrent," *Proceedings of Workshop on Economics of Peer-to-Peer Systems*, 2003.

[15] G. Cote, B. Erol, M. Gallant, and F. Kossentini, "H.263+: Video Coding at Low Bit Rates," *IEEE Trans. on Circuits and Systems for Video Technology*, 1998.

[16] T. M. Cover and J. A. Thomas, *Elements of Information Theory.* New York: John Wiley and Sons, 1991.

[17] G. Daily, "MSNBC makes mess of democratic debate webcast," *StreamingMedia.com*, Feb 2008.

[18] S. Draper and E. Martinian, "Compound conditional source coding, Slepian-Wolf list decoding, and applications to media coding," *Proc. International Symposium on Information Theory*, 2007.

[19] G. D. Forney, "Coset Codes-Part I: Introduction and Geometrical Classification," *IEEE Trans. on Information Theory*, 1988.

[20] ——, "Coset Codes-Part II: Binary Lattices and Related Codes," *IEEE Trans. on Information Theory*, 1988.

[21] B. Girod, A. Aaron, S. Rane, and D. Rebollo-Monedero, "Distributed video coding," in *Proceedings of the IEEE*, 2005.

[22] M. Goodman, "2007 Internet Video Forecast: Moving Beyond YouTube," *Yankee group*, 2007.

[23] C. Guillemot, F. Pereira, L. Torres, T. Ebrahimi, R. Leonardi, and J. Ostermann, "Distributed Monoview and Multiview Video Coding: Basics, Problems and Recent Advances," *IEEE Signal Processing Magazine*, 2007.

[24] L. Guo, S. Chen, Z. Xiao, E. Tan, X. Ding, and X. Zhang, "Measurements, analysis and modeling of bittorrent-like systems," in *Proceedings of ACM Internet Measurement Conference*, Oct. 2005.

[25] B. G. Haskell, A. Puri, and A. N. Netravali, *Digital Video: An Introduction to MPEG-2.* Kluwer Academic Publishers, 1996.

[26] D. Kaplan, "Oprah web show crashes on huge audience," *New York Post*, Mar. 2008.

[27] L. Liang, P. Salama, and E. Delp, "Unequal error protection using Wyner-Ziv coding for error resilience," *Proc. Visual Communications and Image Processing*, 2007.

[28] S. Lin, D. Costello, and M. Miller, "Automatic-repeat-request error-control schemes," *IEEE Communications Magazine*, vol. 22.

[29] F. J. Macwilliams and N. J. A. Sloane, *The Theory of Error Correcting Codes.* Elseiver-North-Holland, 1977.

[30] S. McCanne, V. Jacobson, and M. Vetterli, "Receiver-driven layered multicast," in *Proceedings of ACM SIGCOMM*, Aug. 1996.

[31] W. Norton, "Internet video: the next wave of massive disruption to the U.S. peering ecosystem," *Clean Slate Networking Research Workshop*, 2007.

[32] V. Padmanabhan, H. Wang, P. Chou, and K. Sripanidkulchai, "Distributing streaming media content using cooperative networking," *Proceedings of International Workshop on Network and Operating Systems Support for Digital Audio and Video*, May. 2002.

[33] V. Pai, K. Kumar, K. Tamilmani, V. Sambamurthy, and A. Mohr, "Chainsaw: Eliminating trees from overlay multicast," *Proceedings of International Workshop on Peer-to-Peer Systems*, 2005.

[34] J. Pouwelse, P. Garbacki, D. Epema, and H. Sips, "The Bittorrent P2P file-sharing system: Measurements and analysis," in *Proceedings of International Workshop on Peer-to-Peer Systems*, Feb. 2005.

[35] J. Pouwelse, P. Garbacki, J. Wang, A. Bakker, J. Yang, A. Iosup, D. Epema, M. Reinders, M. van Steen, and H. Sips, "Tribler: A social-based peer-to-peer system," in *Proceedings of International Workshop on Peer-to-Peer Systems*, Feb. 2006.

[36] S. Pradhan and K. Ramchandran, "Distributed Source Coding Using Syndromes (DISCUS): Design and Construction," in *Proceeding of Data Compression Conference*, Mar. 1999.

[37] R. Puri, A. Majumdar, and K. Ramchandran, "PRISM: A video coding paradigm with motion-estimation at the decoder," *IEEE Trans. on Image Processing*, 2007.

[38] D. Qiu and R. Srikant, “Modeling and performance analysis of BitTorrent-like peer-to-peer networks,” *ACM SIGCOMM*, 2004.

[39] D. Schonberg, “Practical Distributed Source Coding and Its Application to the Compression of Encrypted Data,” *Ph.D. thesis*, 2007.

[40] A. Sehgal, A. Jagmohan, and N. Ahuja, “Wyner-ziv Coding of Video: An Error-Resilient Compression Framework,” *IEEE Trans. on Multimedia*, 2004.

[41] E. Setton and J. Apostolopoulos, “Towards Quality of Service for Peer-to-Peer Video Multicast,” *Proceedings of International Conference on Image Processing*, Sep. 2007.

[42] C. Shirky, “What is p2p... and what isntt,” *OReilly Network*, 2000. [Online]. Available: http://www.oreillynet.com/pub/a/p2p/2000/11/24/shirky1-whatisp2p.html

[43] D. Slepian and J. K. Wolf, “Noiseless Coding of Correlated Information Sources,” *IEEE Trans. on Information Theory*, 1973.

[44] T. Stockhammer, M. Hannuksela, and T. Wiegand, “H. 264/AVC in wireless environments,” *IEEE Trans. Circuits and Systems for Video Technology*, vol. 13.

[45] U. Wachsmann, R. Fischer, and J. Huber, “Multilevel Codes: Theoretical Concepts and Practical Design Rules,” *IEEE Trans. on Information Theory*, vol. 45, pp. 1361–1391, Jul. 1999.

[46] H. Wang, N. Cheung, and A. Ortega, “A framework for adaptive scalable video coding using Wyner-Ziv techniques,” *EURASIP Journal on Applied Signal Processing*, 2006.

[47] J. Wang, A. Majumdar, K. Ramchandran, and H. Garudadri, “Robust video transmission over a lossy network using a distributed source coded auxiliary channel,” *Proc. Picture Coding Symposium*, 2004.

[48] T. Wiegand, G. J. Sullivan, G. Bjntegaard, and A. Luthra, “Overview of the H.264/AVC video coding standard,” *IEEE Trans. on Circuits and Systems for Video Technology*, 2003.

[49] J. Wong, “Enhancing collaborative content delivery with helpers,” *Master’s thesis, Univeristy of British Columbia*, Nov. 2004.

[50] A. D. Wyner and J. Ziv, “The Rate-Distortion Function for Source Coding with Side Information at the Decoder,” *IEEE Trans. on Information Theory*, 1976.

[51] Q. Xu and Z. Xiong, “Layered Wyner-Ziv video coding,” *IEEE Trans. on Image Processing*, 2006.

[52] R. Zamir, “The rate loss in the Wyner-Ziv problem,” *IEEE Trans. Information Theory*, vol. 42, pp. 2073–2084, 1996.

[53] M. Zhang, J. Luo, L. Zhao, and S. Yang, “A peer-to-peer network for live media streaming using a push-pull approach,” *Proceedings of ACM International Conference on Multimedia*, 2005.